Science of the Total Environment 808 (2022) 151988

Contents lists available at ScienceDirect

Science of the Total Environment

journal homepage: www.elsevier.com/locate/scitotenv

The developing zebrafish kidney is impaired by *Deepwater Horizon* crude oil early-life stage exposure: A molecular to whole-organism perspective

Fabrizio Bonatesta [a,*], Cameron Emadi [a], Edwin R. Price [a], Yadong Wang [b], Justin B. Greer [c], Elvis Genbo Xu [d], Daniel Schlenk [e], Martin Grosell [f], Edward M. Mager [a]

[a] Department of Biological Sciences and the Advanced Environmental Research Institute, University of North Texas, Denton, TX, USA
[b] Department of Environmental and Occupational Health Sciences, University of Washington, Seattle, WA, USA
[c] Western Fisheries Research Center, United States Geological Survey, Seattle, WA, USA
[d] Department of Biology, University of Southern Denmark, Odense, Denmark
[e] Department of Environmental Sciences, University of California, Riverside, CA, USA
[f] Rosenstiel School of Marine and Atmospheric Science, University of Miami, Miami, FL, USA

HIGHLIGHTS

- Oil exposure induced transcriptional and morphological effects in the pronephros.
- Osmotic challenges revealed impaired water regulation evident by increased edema.
- Pronephric defects from oil exposure have implications for larval osmoregulation.

GRAPHICAL ABSTRACT

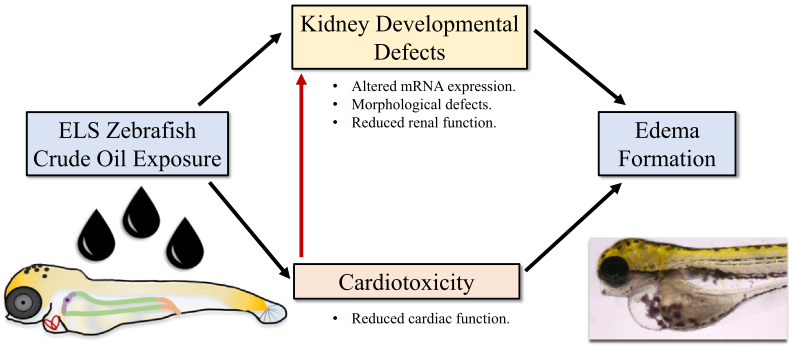

ARTICLE INFO

Article history:
Received 18 October 2021
Received in revised form 22 November 2021
Accepted 22 November 2021
Available online 26 November 2021

Editor: Jay Gan

Keywords:
Pronephros
Osmoregulation
Cardiotoxicity
Edema
Deepwater Horizon
Crude oil

ABSTRACT

Crude oil is known to induce developmental defects in teleost fish exposed during early life stages (ELSs). While most studies in recent years have focused on cardiac endpoints, evidence from whole-animal transcriptomic analyses and studies with individual polycyclic aromatic hydrocarbons (PAHs) indicate that the developing kidney (i.e., pronephros) is also at risk. Considering the role of the pronephros in osmoregulation, and the common observance of edema in oil-exposed ELS fish, surprisingly little is known regarding the effects of oil exposure on pronephros development and function. Using zebrafish (*Danio rerio*) ELSs, we assessed the transcriptional and morphological responses to two dilutions of high-energy water accommodated fractions (HEWAF) of oil from the *Deepwater Horizon* oil spill using a combination of qPCR and whole-mount *in situ* hybridization (WM-ISH) of candidate genes involved in pronephros development and function, and immunohistochemistry (WM-IHC). To assess potential functional impacts on the pronephros, three 24 h osmotic challenges (2 hypo-osmotic, 1 near iso-osmotic) were implemented at two developmental time points (48 and 96 h post fertilization; hpf) following exposure to HEWAF. Changes in transcript expression level and location specific to different regions of the pronephros were observed by qPCR and WM-ISH. Further, pronephros morphology was altered in crude oil exposed larvae, characterized by failed glomerulus and neck segment formation, and straightening of the pronephric tubules. The osmotic challenges at 96 hpf greatly exacerbated edema in both HEWAF-exposed groups regardless of osmolarity. By contrast, larvae at 48 hpf exhibited no edema prior to the osmotic challenge, but previous HEWAF exposure elicited a concentration-response increase in

* Corresponding author at: Department of Biological Science & Advanced Environmental Research Institute, University of North Texas, 1155 Union Circle #310559, Denton, TX 76203-5017, USA.
E-mail address: fabriziobonatesta@my.unt.edu (F. Bonatesta).

http://dx.doi.org/10.1016/j.scitotenv.2021.151988

edema at hypo-osmotic conditions that appeared to have been largely alleviated under near iso-osmotic conditions. In summary, ELS HEWAF exposure impaired proper pronephros development in zebrafish, which coupled with cardiotoxic effects, most likely reduced or inhibited pronephros fluid clearance capacity and increased edema formation.

1. Introduction

The exploration, extraction and transport of crude oil continues to present significant risks of accidental spills in the environment that can range from small spills to large-scale disasters, such as the 2010 *Deepwater Horizon* (DWH) oil spill (Eckle et al., 2012). As such, crude oil is widely studied as a toxicant, especially in the aquatic environment. Its chemical composition and toxicity can vary based on its source (Jung et al., 2013; Perrichon et al., 2016; Li et al., 2019), and can undergo significant changes over time due to weathering processes (Esbaugh et al., 2016). In general, crude oil is characterized by a multitude of different organic molecules, including hydrocarbons. Of these, the polycyclic aromatic hydrocarbons (PAHs) are considered to be the most important drivers of crude oil toxicity, specifically in fish (Forth et al., 2017). Aside from direct mortality, various sub-lethal effects have been reportedly associated with aquatic crude oil exposure (Li et al., 2021), which likely contribute to negative effects at the individual and population levels (Grosell and Pasparakis, 2021). Among the most studied of these effects in fish is a syndrome of cardiotoxic effects during the sensitive early life stages (ELS) largely characterized by impaired fluid regulation as indicated by the presence of pericardial and yolk sac edema (Incardona et al., 2004).

Recent transcriptomics studies performed on ELS mahi-mahi (Xu et al., 2016) and red drum (Xu et al., 2017) exposed to DWH crude oil have shed light on additional pathways affected by crude oil exposure in fish, aside from the widely recognized cardiotoxicity. Some tissues and pathways that appear to be affected are the peripheral nervous system (important for olfaction, vision, hearing and mechanosensing: Magnuson et al., 2018; Schlenker et al., 2019), central nervous system (e.g., behavioral effects: Khursigara et al., 2018), cholesterol biosynthesis (McGruer et al., 2019), hepatocyte proliferation, and kidney development (Xu et al., 2016; Xu et al., 2017). Given these are relatively new discoveries, few studies have been conducted to examine these affected pathways (Magnuson et al., 2018; Schlenker et al., 2019), and despite the importance of a functional kidney, there are almost no studies that have examined the potential nephrotoxicity of crude oil exposure. In fact, in addition to the transcriptomic studies previously mentioned, only a single study has speculated on the potential effects of crude oil on the ELS teleost kidney (known as the pronephros). Specifically, Incardona et al. (2004) revealed that ELS exposure of zebrafish (*Danio rerio*) to phenanthrene, a 3-ringed PAH present in crude oil, altered the gross morphology of the developing pronephros.

The kidney is an important osmoregulatory organ, and plays a role in ion and water regulation (Larsen et al., 2014). The nephron is the functional unit of the kidney and is indispensable to maintaining internal homeostasis in adult fish and, putatively, during ELSs (Kersten and Arjona, 2016). Specifically, while the integument of ELS fishes plays a role in water and ion regulation initially, the pronephros, nevertheless, seems to become functional relatively early (Hentschel et al., 2007; Rider et al., 2012), even before the gills begin to function. This has been mostly studied in zebrafish, where the gills do not become functional until 7 days post fertilization (dpf) (Rombough, 2002), and a functional pronephros is observed around 48 h post fertilization (hpf; Drummond et al., 1998). Given the importance of the pronephros clearance capacity for ELS fish, any factors affecting the excretory ability of the pronephros could result in liquid accumulation in fish larvae (Rider et al., 2012). Consequently, failure of zebrafish pronephros development and/or function, induces the presence of a pericardial and yolk-sac edema in zebrafish at around 72 hpf (Kramer-Zucker et al., 2005b; Perner et al., 2007), which is a sign of impaired water volume regulation and impaired osmoregulation more generally. As mentioned previously, this is also a phenotype that is observed in crude oil exposed ELS fishes (Incardona and Scholz, 2016). Further, the pronephros requires a properly functioning cardiovascular system to develop a functional glomerulus (the filtration apparatus of the pronephros); thus, crude oil induced cardiotoxicity may influence glomerulogenesis in exposed fish. Indicatively, Serluca et al. (2002) demonstrated that zebrafish larvae lacking a heartbeat - and therefore hemodynamic forces - fail glomerular formation. Therefore, crude oil-induced cardiotoxicity warrants consideration as a factor for pronephric developmental defects in addition to potential direct effects of crude oil exposure (Rider et al., 2012; Incardona and Scholz, 2016).

Among teleosts, nephron structure can vary based on the osmoregulatory needs incurred by their environment, ranging from a more complex structure in freshwater fishes (designed to clear excess fluid accumulation associated with living in a dilute environment) to the simpler (including aglomerular) structures found in marine fishes (McDonald, 2007). Despite these differences, nephrogenesis appears to share similar defined stages, listed here in order: the specification of mesodermal cells; the onset of epithelization of the nephron; the continued genesis and patterning of the nephron with subsequent specialization and expansion of each nephric segment; and the onset of nephric blood supply (including glomerular filtration) due to the formation of nearby vasculature (Drummond, 2005; Gerlach and Wingert, 2013; Outtandy et al., 2019). All of these stages are induced and guided by genetic programs involved in cell fate specification and migration (Ma and Jiang, 2007; Vasilyev et al., 2009), which ultimately lead to nephron formation, and which are believed to be shared among vertebrates (Outtandy et al., 2019). Some of the genes directly or indirectly involved in pronephros development are highlighted in Table S1, in addition to the zebrafish pronephric structure depicted in Fig. S1. Morphologically, once fully formed, the zebrafish pronephros has a basic structure. It is composed of a single glomerulus and two parallel nephrons. The glomerulus is composed of podocytes and a capillary tuft, while each nephron is made of a neck segment, a pronephric tubule (divided into 4 segments) and a pronephric duct (Gerlach and Wingert, 2013). The zebrafish pronephros is considered fully functional at the onset of glomerular filtration, which is believed to occur around 48 hpf (Drummond et al., 1998). Any interference during this tightly regulated developmental processes could result in defects associated with pronephros morphology and function (Gerlach and Wingert, 2013).

Based on this information, the general objective of this study was to examine the effects of DWH crude oil exposure on freshwater teleost kidney development. We addressed this objective by focusing on 1) quantifying and characterizing the transcriptional responses of genes involved in zebrafish pronephros development and function, 2) analyzing morphological pronephros abnormalities induced by crude oil exposure, and 3) assessing osmoregulatory responses of fish previously exposed to DWH crude oil by using osmotic challenge tests. The results of this study address a key knowledge gap in our understanding of the contributions of impaired renal function to the toxicity of crude oil exposures in ELS fish.

2. Methods

2.1. Experimental design

Two separate tests were performed. The first test (Test 1) was performed to collect samples for real-time quantitative polymerase chain reaction (qPCR) analysis and the first osmotic challenge test (described later). The second test (Test 2) was performed to collect samples for whole-mount *in situ* hybridization (WM-ISH), whole-mount immunohistochemistry (WM-IHC) and the second osmotic challenge test. Methods used were

the same among tests unless indicated differently. Refer to Fig. S2 for a graphical display of the experimental design.

2.2. HEWAFs preparation and analysis

Stock solutions of high-energy water accommodated fractions (HEWAFs) of DWH slick oil OFS (oil from surface) were prepared daily with Embryo (E3) medium ($CaCl_2.2H_2O$ 0.33 mM, $MgSO_4$ 0.33 mM, NaCl 5 mM, KCl 0.17 mM, in 1 L of Milli-Q water: Bai et al., 2010). Crude oil samples OFS-20100719-JUNIPER-001 (A0091G and A0087Q) were used for Tests 1 and 2, respectively. HEWAFs were prepared at an oil loading rate of 1 g/L as previously described (Incardona et al., 2013; Forth et al., 2017). Briefly, after mixing for 30 s on low in a 3-speed commercial food blender with a 1-gal (3.8-L) stainless steel container (Waring CB15, Waring Commercial, Torrington, CT), the WAF was transferred to a separatory funnel, capped, and covered from direct light for 1 h. Subsequently, the lower ~90% of the WAF stock solution was collected and used for the preparation of experimental solutions. With each HEWAF preparation, a sample of the 40% HEWAF dilution was collected and held at 4 °C until analysis. Extraction and GC/MS-SIM analysis of PAHs were performed by ALS Environmental (Kelso, WA) according to USEPA methods 3510C and 8270D, respectively. Reported ΣPAH concentrations represent the sum of 50 select PAH analytes. Sum PAH concentrations for the 20% HEWAF were estimated by simply dividing the measured concentrations for the corresponding 40% HEWAF preparations by two.

2.3. HEWAF exposure

Zebrafish (*Danio rerio*) embryos were obtained from the wild-type AB zebrafish brood stock at the University of North Texas (IACUC protocol #19-016) which was purchased from a local store (Fish n' Chirps Pet Center, Denton, TX). HEWAF dilutions were prepared using E3 medium for nominal test solutions of 0%, 20% and 40%. 96 h exposures were performed using 200 mL of test solution in 250 mL crystalizing dishes and initiated with the addition of zebrafish embryos at approximately 2 hpf. For Test 1 only, larvae were transferred to clean control E3 medium for an additional 3 days of recovery following the 96 h HEWAF exposure. Water changes (>80%) were performed daily using dilutions of a freshly prepared HEWAF each day for the full experiment duration. Test 1 started with 14 dishes for 0% HEWAF (control), 14 dishes for 20% HEWAF and 18 dishes for 40% HEWAF; 50 embryos were loaded per dish. Test 2 started with 9 dishes for 0% HEWAF (control), 2 dishes for 20% HEWAF and 13 dishes for 40% HEWAF; 40 embryos were loaded per dish. Exposure dishes were placed in an environmental chamber set to 28 °C during the duration of the tests. Temperature, dissolved oxygen (DO), and pH were recorded daily using a YSI ProODO oxygen meter (YSI Incorporated, Yellow Springs, OH) for temperature and DO, and an Orion Star A121 portable pH meter (Thermo Fisher Scientific, Waltham, MA) for pH.

2.4. Phenanthrene exposure

A separate set of zebrafish embryos were exposed to phenanthrene (PHN), >99.5 purity, (Sigma-Aldrich, St. Louis, MO) for WM-IHC analysis. A 10 mg/mL stock PHN solution was prepared in dimethyl sulfoxide (DMSO) and diluted in E3 medium to a 56 μM (9.98 mg/L) concentration (0.1% DMSO). The test was performed in triplicate in a plastic 12 well cell culture plate with a lid on and with 2.5 mL solution per well. It is important to note that this concentration likely exceeds the solubility limit for PHN (Verschueren, 2001); however, our goal was to simply replicate the exposure as described by Incardona et al. (2004) to serve as a positive control for inducing PAH mediated defects to the developing pronephros. These authors stated that "It was empirically determined (data not shown) that high nominal concentrations were required to maintain steady aqueous levels due to the small exposure volumes and high PAH-binding capacity of the tissue culture plastic". An E3 medium control group and a 0.1% DMSO (in E3 medium) control were also included. 10 embryos per well were exposed to each solution starting at ~5 hpf up until 72 hpf in an incubator at 28 °C. Test solutions were changed daily (>80%).

2.5. Sample collection and cDNA synthesis

Zebrafish whole embryos/larvae were randomly collected at 48 and 96 hpf from the Test 1 HEWAF exposure for mRNA isolation. Specifically, 5–6 replicates of 20 embryos/larvae were sampled per each concentration and time point. 6 replicates of 10 larvae each were also collected following 3 days of recovery (7 dpf) in control media, however only 3 replicates were collected from those previously exposed to the highest HEWAF concentration (40%) due to high mortality. Embryos/larvae were collected and stored in RNAlater (Invitrogen, Waltham, MA) solution at 4 °C. Samples were later homogenized with a tissue disperser (IKA Works, Wilmington, NC) in TRIzol® (Life Technologies, Carlsbad, CA). Total RNA isolation was performed with the Maxwell® 16 Instrument and the corresponding Maxwell® 16 LEV simplyRNA Tissue Kit (Promega Corporation, Madison, WI) following the manufacturer's protocol. Isolated total RNA was quantified and assessed for purity using a NanoDrop (Thermo Fisher Scientific, Waltham, MA) and the RNA integrity was confirmed by gel electrophoresis. 1 μg of each total RNA sample was incubated using the ezDNase™ enzyme (Invitrogen, Waltham, MA) to digest any potential gDNA and then reverse transcribed into cDNA using SuperScript™ IV VILO™ (SSIV VILO) Master Mix (Invitrogen, Waltham, MA). Final cDNA products were diluted tenfold in RNAse free water and stored at −20 °C before use.

2.6. Transcript selection and primer design

The mRNA transcripts analyzed in this study were selected based on their expression domains within the pronephros, specifically their association with the glomerulus (podocytes and capillary tuft), neck segments, pronephric tubules and ducts, as well as the role they play during pronephros development and pronephric function, specifically transcription factors and structural or functional proteins (Table S1). Transcripts related to nephrotoxicity interpreted by Xu et al. (2016) and (2017) with the ingenuity pathways analysis are associated with the mammalian kidney. Given that some physiological activities of the mammalian kidney are performed by the gills in fish (Larsen et al., 2014), only *bmp4* was selected from the previously mentioned transcriptomic studies, given its involvement in zebrafish pronephric development (Weber et al., 2008). Zebrafish primers were designed to amplify a PCR product of ~100 bp based on the following zebrafish sequences from GenBank: *bmp4* U82231.1, *cdh17* AF428098.1, *clc-K* NM_200382.1, *flk-1* or *vegfr2* U75995.1, *mmp2* NM_198067.1, *mmp9* AY151254.1, *nephrin* NM_001040687.1, *pax2.1* AF067530.1, *podocin* DQ466905.1, *sim-1* NM_178222.3, *slc20a1a* NM_213179.1, *vegf* AF016244.1, *wt1a* NM_131046.1, *wt1b* NM_001039634.2, *mob4* NM_001003439.1, *lsm12b* NM_213148.1, *ef1α* FJ915061.1, *b-actin2* NM_181601.5, *rpl13a* NM_212784.1. Primers are listed in Table S3.

2.7. qPCR analysis

qPCR was performed using an Agilent AriaMx Real-time PCR System instrument (Agilent, Santa Clara, CA) and Power SYBR Green Master Mix (Thermo Fisher Scientific, Waltham, MA). Reactions were performed in 96 well plates using 6 μL sterile water, 10 μL SYBR Green, 1 μL of each forward and reverse primer (to final concentrations of 0.5 μmol L^{-1} each) and 2 μL of diluted cDNA for a final volume of 20 μL per reaction. Settings were as follows: hot start at 95 °C for 3 min, followed by 40 amplification cycles at 95 °C for 5 s and 60 °C for 10 s. Specificity of each primer pair was initially verified by gel electrophoresis and sequencing, and subsequently confirmed for each reaction using a terminal melting curve analysis. Each plate contained all replicates for each time point and WAF treatments, and were run in duplicate. The PCR Miner software (Zhao and Fernald, 2005) was used to analyze the raw data and obtain Ct values and reaction efficiencies (E) for each individual reaction. These values were then used to calculate initial fluorescence values (R_0) according to the equation: R_0 =

$(1 + E)^{Ct}$. Mean R_0 values were then used to normalize all target gene mRNA expression levels to the geometric mean of 4 selected housekeeping genes (*ef1a, lsm12b, b-actin2, rpl13a*) as previously described (Vandesompele et al., 2002). Normalized R_0 values were then expressed relative to the lowest expressed mean value across all time points and treatments (Zhao and Fernald, 2005).

2.8. Synthesis of RNA probes for WM-ISH

Primers were designed with a T7 promoter region added to the reverse primer (Table S4). The sequences for *bmp4* (868 bp), *clc-K* (797 bp), *vegfr2* (789 bp), *pax2.1* (807 bp), *sim-1* (787 bp), *wt1a* (801 bp), *slc20a1a* (1002 bp) were then amplified by PCR. Specific DIG-labeled RNA probes were synthesized (Roche, Basel, Switzerland) for each gene of interest according to the manufacturer's instructions using PCR products. Sense RNA probes for each sequence were also synthesized.

2.9. Whole-mount in situ hybridization (WM-ISH)

WM-ISH analyses targeted only those transcripts that manifested in altered mRNA expression due to crude oil exposure by qPCR, with the exception of *podocin* for which no successful probes were synthesized despite multiple attempts. The protocol was performed based on the instructions provided by Thisse and Thisse (2008). Zebrafish embryos and larvae were collected every 24 h for the duration of the HEWAF exposure (96 h) from Test 2 only. Sample sizes were as follows: 4–7 embryos were examined per treatment (0% and 40% HEWAF only) at 24 hpf; 4–11 embryos/larvae at 48 hpf; 7–10 larvae at 72 hpf; 6–11 larvae at 96 hpf. If needed, chorions were removed manually from embryos ≤48 hpf using forceps under a dissecting microscope before collection. Critical steps and modifications of the protocol are as follows: to remove pigments, larvae were incubated in 3% H_2O_2/ 0.5% KOH in PBS until larvae did not show any pigments, and then washed in 1× PBS; samples were digested in 10 μg/mL proteinase K (Invitrogen, Waltham, MA) in PBST with different incubation times (24 hpf embryos for 5 min, 48 hpf embryos for 15 min, 72 and 96 hpf larvae for 30 min); samples were hybridized overnight in hybridization media (50% Formamide, 5× standard sodium citrate -SSC-, Tween20 0.1%, citric acid to pH 6.0, 50 μg/mL heparin, 500 μg/mL yeast tRNA) containing antisense DIG-labeled RNA probe (1.5 ng/μL); samples were incubated overnight at 4 °C with gentle shaking to immune react with alkaline phosphatase–coupled anti-DIG antibodies (Roche, Basel, Switzerland) diluted 1:3000 in blocking reaction solution (MABT/10% goat serum/20% block reagent); samples were stained in the dark in BM purple substrate (Roche, Basel, Switzerland) with 5 mM levamisole until satisfactory staining occurred (checked every 30 min using a dissecting microscope). If the reaction took longer than 6 h, samples were placed at 4 °C overnight. Pictures were taken using a Leica S9D stereo microscope and a Leica MC190 HD microscope camera (Leica, Wetzlar, Germany). Only lateral photos of WH-ISHs are presented, as it was difficult to observe the staining from dorsal and ventral views due to the presence of the yolk-sac. 96 hpf zebrafish larvae were similarly processed using a sense DIG-labeled RNA probe, and samples for each time point were also processed without using any DIG-labeled RNA probe as negative controls.

2.10. Whole-mount immunohistochemistry (WM-IHC)

The WM-IHC procedure was adapted from previously published methods (Incardona et al., 2004; Dent et al., 1989). Briefly, 72 hpf zebrafish larvae were randomly collected from 0%, 20% and 40% HEWAF solutions (from Test 2 only) and 56 μM (9.98 mg/L) PHN solution (n = 8–11). Larvae were fixed in Fixative (20% DMSO/ 80% MeOH) for 2 h at RT. To remove pigmentation, fixation continued in 10% H_2O_2 in Fixative for 2 days. Samples were then incubated in 100% MeOH at −20 °C until use. Larvae were washed in a graded series of MeOH/PBS and permeabilized for 1 h in Blocking Solution (PBS, TritonX-100 0.2%, DMSO 1%, goat serum 5%) at RT. Samples were then incubated in monoclonal antibody α6F hybridoma supernatant (DSPH, University of Iowa, Iowa City, IA) (antigen = ATPase, Na^+ K^+ alpha-1 subunit) diluted 1:10 in Blocking solution overnight at 4 °C with gentle shaking. Larvae were then washed for 3 × 1 h in PBS/ 0.2% TritonX-100 at RT, and incubated at 4 °C with the secondary antibody, AlexaFluor488-conjugated goat anti-mouse IgG (α6F) (Molecular Probes, Eugene, OR) diluted 1:1000 in Blocking Solution. This was followed by 3 × 1 h washes in PBS/ 0.2% TritonX-100 at RT, after which larvae were mounted on concave depression cavity glass microscope slides in 50% glycerol/ 50% PBS for microscope analysis and picture capture. Pictures and z-scans of the larvae with various magnifications were obtained by using a Zeiss Axiovert 200 M optical microscope (Zeiss, Oberkochen, Germany) with a Yokogawa CSU10 spinning disk confocal attachment (Yokogawa, Tokyo, Japan). Pictures and z-scans were finally processed with ImageJ NIH software to produce clearer pictures of the pronephros.

2.11. Osmotic challenge tests

Two 24 h osmotic challenge tests were performed after HEWAF exposure (Fig. S3): one starting at 96 hpf and ending at 120 hpf (larvae from Test 1), the other starting at 48 hpf and ending at 72 hpf (larvae from Test 2). Three waters varying in osmotic strength were used for the challenge: Milli-Q water, E3 medium, and E3 medium enriched with 25× NaCl concentration (25× NaCl E3 medium). E3 medium represented the control water (albeit hypo-osmotic), Milli-Q water was obtained by using a Barnstead *E*-Pure Water Purification System (APS Water Services Corporation, Lake Balboa, CA) and represented a more severe hypo-osmotic environment, and an enriched E3 medium supplemented with 25× the concentration of NaCl (125 mM NaCl in 1 L) to emulate iso-osmotic conditions (i.e., ~240 mOsm in zebrafish larvae; Kozłowski et al., 2017). pH was adjusted in all water to 7.2 ± 0.1, DO and temperature were measured at the beginning of the test. Zebrafish larvae were randomly transferred from each HEWAF solution (0%, 20% and 40% HEWAF) to 200 mL of the different salinity solutions in 250 mL crystalizing dishes in a fully factorial design. Osmotic challenge Test 1 started with one dish containing 20 larvae for each salinity solution; osmotic challenge Test 2 started with three dishes containing 5 larvae for each salinity solution. Prior to transfer, larvae were gently rinsed twice in their respective salinity solutions. Survival was quantified after the osmotic challenge tests. Pericardial and yolk sac edema and heart rate were quantified after the HEWAF exposure (at 48 hpf and 96 hpf, before each osmotic challenge) and after the osmotic challenge tests (at 72 hpf and 120 hpf, respectively).

2.12. Edema and heart rate quantification

Pictures and 15 s videos of laterally positioned zebrafish larvae were acquired using a Leica S9D stereo microscope and a Leica MC190 HD microscope camera for Test 1 (n = 13–16), and a Nikon SMZ800N stereo microscope (Nikon Instruments Inc., Melville, NY) for Test 2 (n = 9–10). Both sets of analyses were conducted within the same environmental chamber as for the exposures to maintain constant temperature. Larvae were mounted in 3% methylcellulose prepared with the respective waters (Milli-Q water, E3 medium, 25× NaCl E3 medium) at RT. Heart rates were determined by counting the number of ventricular beats per 15 s by playing the video at reduced speed, and multiplying that number by 4 to obtain the number of beats per minute. Pericardial and yolk sac edema area was measured according to the protocol provided by Edmunds et al., 2015 using ImageJ NIH software.

2.13. Statistical analysis

Data are presented as means ± standard error of the mean (SEM). Statistical analyses were performed using SigmaPlot 12.3 (Systat Software, Inc., San Jose, CA). Differences in mRNA expression were assessed by two-way ANOVA (time and HEWAF treatment considered as factors) followed by Holm-Sidak post hoc test. If normality or equal variance failed, data transformation was performed. Specifically, *pax2.1*, *vegf*, *vegfr2*, *sim-1*

data were ln-transformed, and a square root transformation was performed for *cdh17* data. No adequate transformation was found for *mmp-9* data and a one-way ANOVA followed by Holm-Sidak post hoc test was performed instead, excluding time as a factor. A one-way ANOVA (HEWAF treatment as factor) followed by a Holm-Sidak post hoc test was performed to analyze differences in heart rate at 96 hpf (before osmotic challenge Test 1); given failed normality, a Kruskal-Wallis test (one-way ANOVA on ranks) followed by a Tukey's post hoc test was performed to assess differences in edema size at 96 hpf. Edema area and heart rate data collected after the 24 h osmotic challenge Test 1 failed equal variance and normality, therefore no ANOVA test was performed. A one-way ANOVA (HEWAF treatment as factor) was performed to assess differences in edema area size at 48 hpf (before osmotic challenge Test 2). A Grubbs' test was performed to remove potential outliers in edema area and heart rate data collected after the 24 h osmotic challenge Test 2. Subsequently, two-way ANOVA (HEWAF treatment and water osmolarity considered as factors) followed by Holm-Sidak post hoc test was performed to assess differences. In all cases, differences were considered significant at $P < 0.05$.

3. Results

3.1. Water parameters and PAHs analysis

Initial and final water quality parameters (temperature, pH and DO) were measured daily from each test chamber and are presented as means ± SEM per treatment (Table S2). HEWAF concentrations are presented as the geometric means ± SEM of initial and final values of Σ50 PAH concentrations (Table S2). For Test 1, the measured ΣPAH concentration for the 40% HEWAF was 150.4 ± 26.5 μg/L and therefore the estimated ΣPAH concentration for the 20% HEWAF was 75.2 ± 13.2 μg/L. For Test 2, the measured and estimated concentrations were 467.1 ± 30.1 μg/L and 233.6 ± 15.0 μg/L, respectively. Notably, a wide variance was unexpectedly observed in the ΣPAH concentrations for the HEWAF preparations between Tests 1 and 2. However, the ΣPAH profiles of both HEWAFs (represented as the percentage of ΣPAHs by ring class) were not different (Table S5).

3.2. qPCR analysis of mRNA expression

In terms of the mRNA levels related to the capillary tuft (Fig. 1), 7 dpf zebrafish exposed to 150 μg/L ΣPAH showed a significant increase in expression of *vegf* compared to control fish and fish exposed to the lowest HEWAF dilution (75 μg/L ΣPAH); a significant increase in *vegfr2* expression was also observed in zebrafish exposed to 150 μg/L ΣPAH at 48 hpf (compared to control fish only) and 96 hpf (compared to control fish and fish exposed to 75 μg/L ΣPAH), which returned to the control level at 7 dpf; no significant effect was observed related to *mmp-2* expression; however, a significant spike in expression related to *mmp-9* (compared to control fish and fish exposed to 75 μg/L ΣPAH) was observed with 7 dpf fish exposed to 150 μg/L ΣPAH.

With respect to podocyte expression (Fig. 2), there was a significant increase in *wt1a* expression in 96 hpf zebrafish exposed to 150 μg/L ΣPAH compared to control fish and fish exposed to the lowest HEWAF dilution, but no differences at later time points. Expression of *wt1b* significantly increased in 7 dpf zebrafish exposed to ΣPAH 150 μg/L compared to control fish only. *Podocin* expression significantly decreased in 48 hpf larvae exposed to 150 μg/L ΣPAH compared to control only (which then returned to normal value), while no significant difference was observed related to *nephrin* expression.

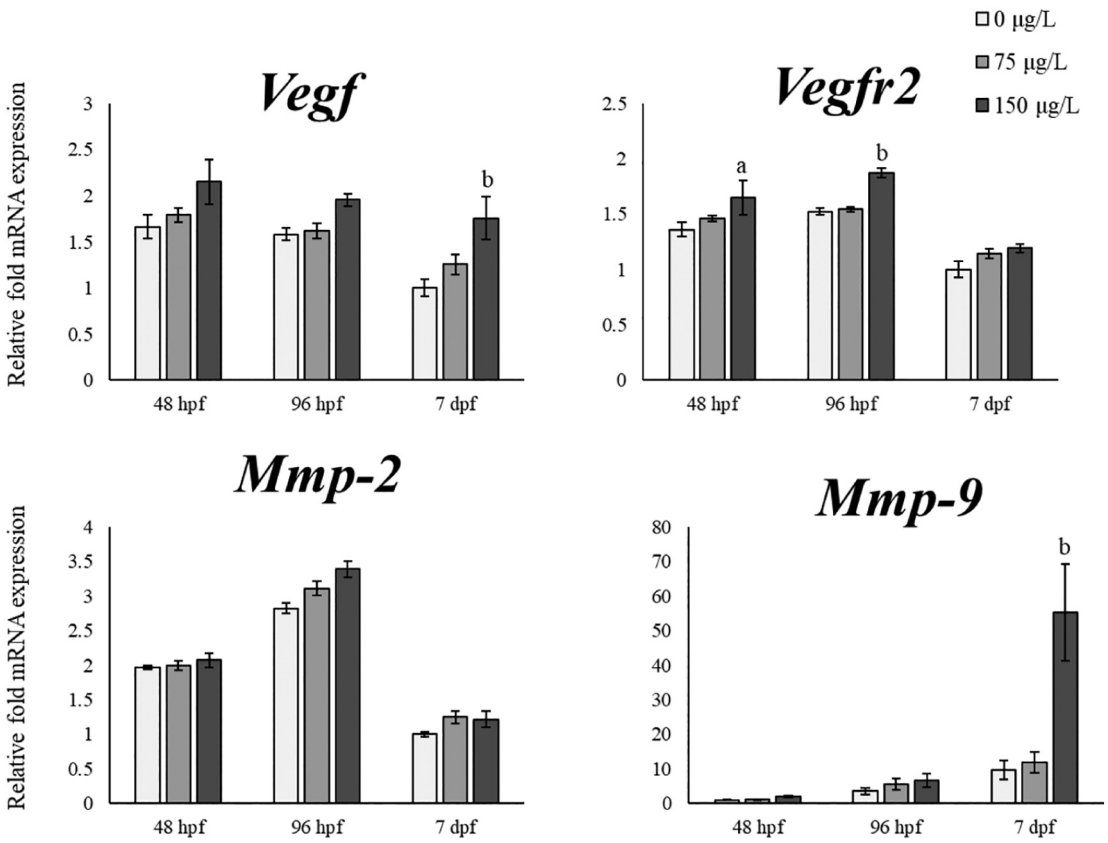

Fig. 1. Relative whole-body mRNA expression levels of transcripts involved in the capillary tuft development and function within the pronephric glomerulus. Transcripts were analyzed in zebrafish during HEWAF exposure (48 and 96 hpf) and after 3 days of recovery in clean control media (7 dpf). $n = 6$ (20 embryos/ larvae each) run in duplicate for 48 and 96 hpf; n = 6 (10 larvae each) run in duplicate for 0 and 75 μg/L ΣPAH at 7 dpf, and $n = 3$ for 150 μg/L ΣPAH at 7 dpf. Error bars represent ± SEM. Differences were considered significant at $P < 0.05$ (a = statistically different than control; b = statistically different than control and other treatment).

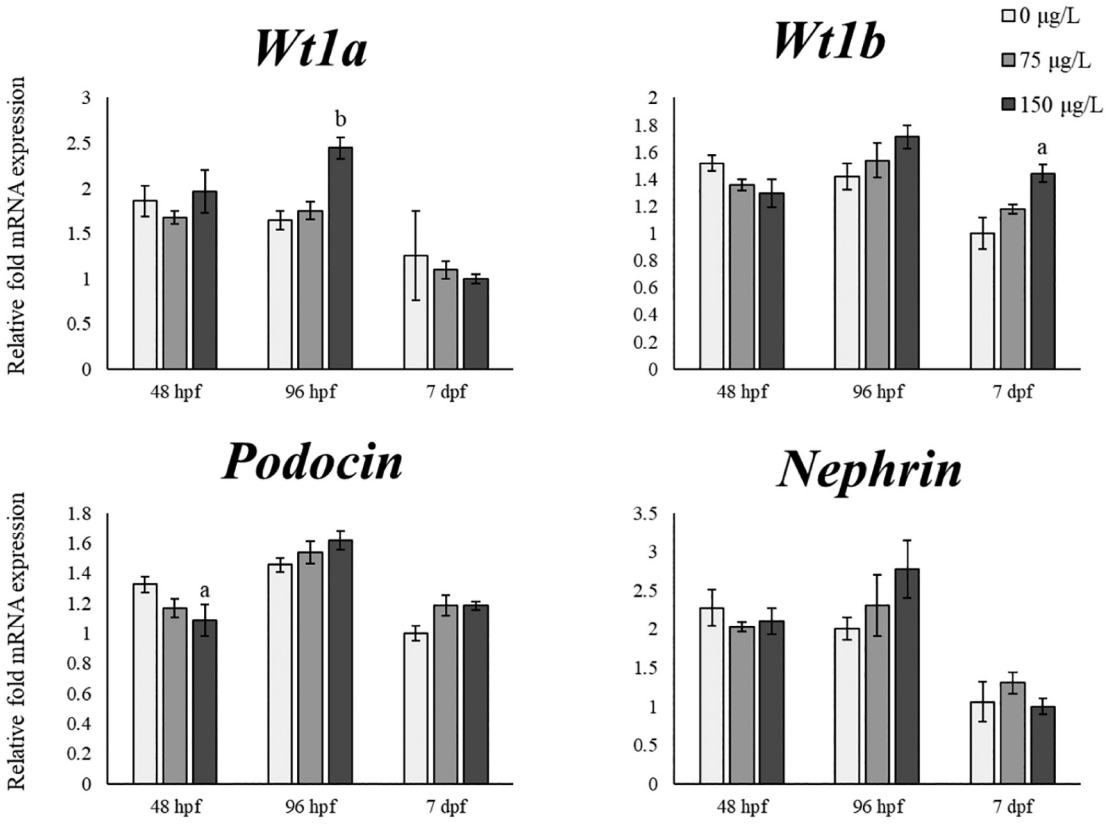

Fig. 2. Relative whole-body mRNA expression level of transcripts involved in podocytes development and function within the pronephric glomerulus. Transcripts were analyzed in zebrafish during HEWAF exposure (48 and 96 hpf) and after 3 days of recovery in clean control media (7 dpf). n = 6 (20 embryos/ larvae each) run in duplicate for 48 and 96 hpf; n = 6 (10 larvae each) run in duplicate for 0 and 75 µg/L ΣPAH at 7 dpf, and n = 3 for 150 µg/L ΣPAH at 7 dpf. Error bars represent ± SEM.Differences were considered significant at $P < 0.05$ (a = statistically different than control; b = statistically different than control and other treatment).

In terms of neck segments, pronephric tubules and ducts (Fig. 3), there was a significant increase in *pax2.1* expression in 48 hpf zebrafish exposed to 150 µg/L ΣPAH compared to control fish only, which then returned to the control level at later time points. A significant increase of *sim-1* expression at 48 hpf and a significant decrease in expression at 7 dpf were observed in zebrafish exposed to 150 µg/L ΣPAH compared to fish exposed to 75 µg/L ΣPAH, but not compared to control fish. *Slc20a1a* expression increased in 96 hpf zebrafish exposed to the lowest HEWAF dilution (75 µg/L ΣPAH) compared to control fish only, which returned to the control level at 7 dpf. An increase in *clc-K* expression was also observed in 96 hpf zebrafish exposed to both HEWAF dilutions compared to control, with no differences at 7 dpf.

Finally, by examining the mRNA expression of other transcripts involved more generally in pronephros development and function (Fig. 4), there was a significant concentration-response increase in *bmp4* expression at 48 and 96 hpf zebrafish, which seemed to recover at 7 dpf; however, no statistically significant differences were observed related to *cdh17* mRNA expression.

3.3. Whole-mount in situ hybridization

Wt1a (Fig. 5A) was expressed on the anterior portion of the developing nephron in control fish at 24 hpf, which then developed into a rounded shape expressed by the glomerulus in later life stages. The expression pattern appeared to be similar in zebrafish exposed to 467 µg/L ΣPAH until 96 hpf, in which the staining appeared more diffuse and elongated suggesting either structural alteration to the glomerulus or ectopic expression. A similar transcript expression pattern was observed for *vegfr2* at 96 hpf (Fig. 5B). However, oil exposed fish lacked a distinct expression of *vegfr2* around the glomerulus at 48 and 72 hpf. *Vegfr2* was also expressed in the vasculature of the trunk (specifically at 24 hpf) and of the cranial area (at all life stages). Crude oil exposed fish showed an altered expression of *vegfr2* at all life stages regarding the vasculature as well.

The expression of *slc20a1a* (Fig. 5C) was visible in the developing nephrons at 24 hpf in control fish. Its expression migrated rostrally and followed the morphological development of the proximal convoluted tubules by finally being expressed in a convoluted fashion at 96 hpf. In 24 hpf crude oil exposed larvae, *slc20a1a* expression was more faint/diffuse compared to the distinct expression in control fish. Further, crude oil exposed fish failed to show expression of *slc20a1a* in a convoluted fashion at 72 and 96 hpf compared to control fish.

In 24 hpf control fish, *pax2.1* (Fig. 5D) was expressed on the majority of the nephron, specifically on tubules and ducts. However, starting at 48 hpf it was expressed singularly on the neck segments, with a very distinct expression at 96 hpf (two distinct segments protruding medially from each tubule). Expression related to the pronephros appeared normal in oil exposed fish at 24, 48 and 72 hpf; however, at 96 hpf, *pax2.1* was only expressed in two single dots in oil exposed fish, instead of the typical extended shape of the neck segments. Importantly, *pax2.1* was not only expressed in the pronephros but also in the midbrain-hindbrain boundary, hindbrain neurons, spinal cord neurons, thyroid primordium, otic vesicles and the eyes (optic stalk and choroid fissure). The expression of *pax2.1* on the hindbrain neurons, spinal cord neurons and eyes appeared normal. However, a less distinctive expression of *pax2.1* was observable related to the thyroid primordium and otic vesicles (from 48 to 96 hpf) and the midbrain-hindbrain boundary (at 96 hpf).

Clc-K (Fig. 5E) was expressed in the duct and the distal tubules (related to the pronephros), but also on the musculature system of the zebrafish at all life stages in control fish. However, the observed expression on the musculature could be related to overstaining, as this staining was never previously reported and using the *clc-K* sense probe induced some minor staining on the head region. In 24 hpf crude oil exposed fish, expression of *clc-K* on the

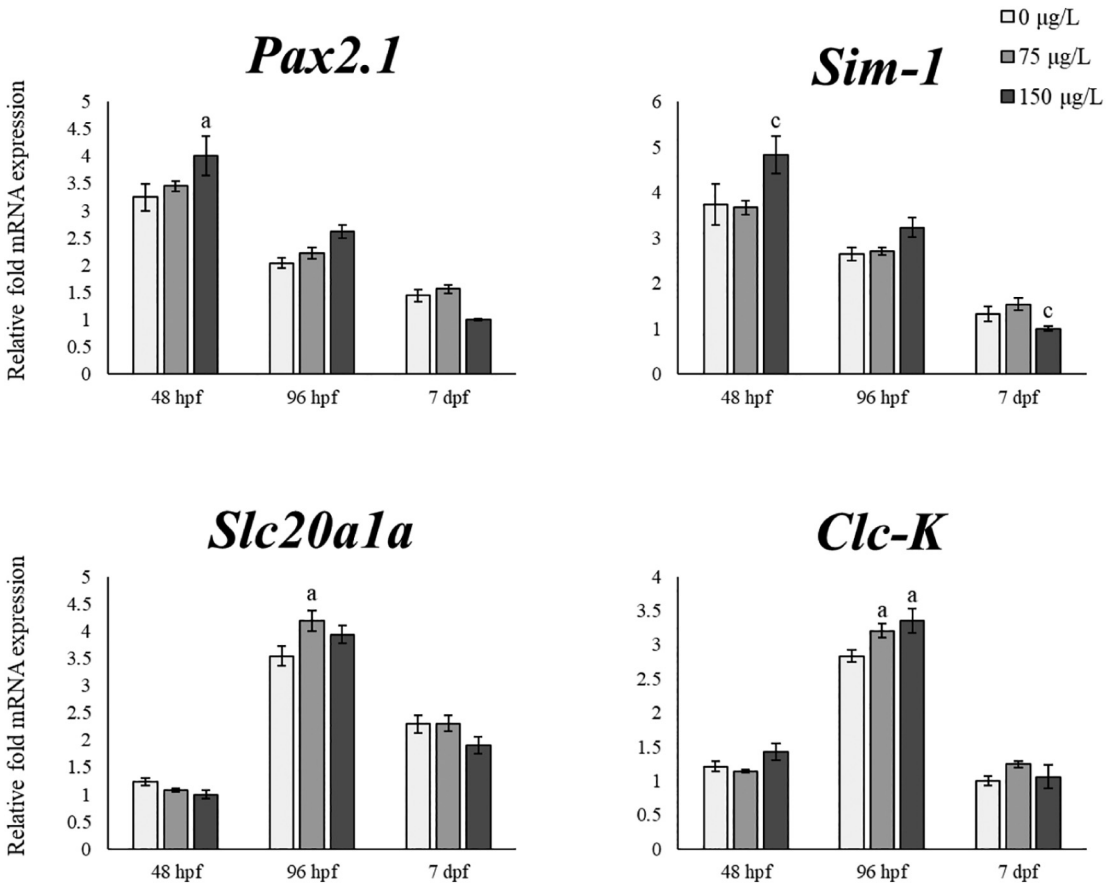

Fig. 3. Relative whole-body mRNA expression level of transcripts involved in neck segments, pronephric tubules and ducts development and function. Transcripts were analyzed in zebrafish during HEWAF exposure (48 and 96 hpf) and after 3 days of recovery in clean control media (7 dpf). n = 6 (20 embryos/ larvae each) run in duplicate for 48 and 96 hpf; n = 6 (10 larvae each) run in duplicate for 0 and 75 µg/L ΣPAH at 7 dpf, and n = 3 for 150 µg/L ΣPAH at 7 dpf. Error bars represent ± SEM. Differences were considered significant at $P < 0.05$ (a = statistically different than control; b = statistically different than control and other treatment; c = statistically different than fish exposed to 75 µg/L ΣPAH only).

ducts appeared to be elongated compared to control fish. *Sim-1* was only clearly expressed on the pronephros at 24 hpf in both control and oil exposed fish (with no major differences). Further, *sim-1* (Fig. 5F) was expressed in control fish on the optic recesses, hypothalamus, posterior tuberculum, pectoral fins and some other unidentified structures around the gills. The morphological expression of *sim-1* on the optic recesses, hypothalamus and posterior tuberculum appeared to differ from control starting at 48 hpf.

Bmp4 (Fig. 5G) was expressed at the cloaca at 24 hpf zebrafish, in both control and oil exposed fish. At 24 hpf, *bmp4* was also expressed on the axial fin fold. In later stages (48 to 96 hpf), its expression was observed on the heart, otic vesicles, and swim bladder (at 96 hpf only). The expression of *bmp4* on all these structures was noticeably altered in crude oil exposed zebrafish starting from 72 hpf, characterized by a non-specified and indistinct staining.

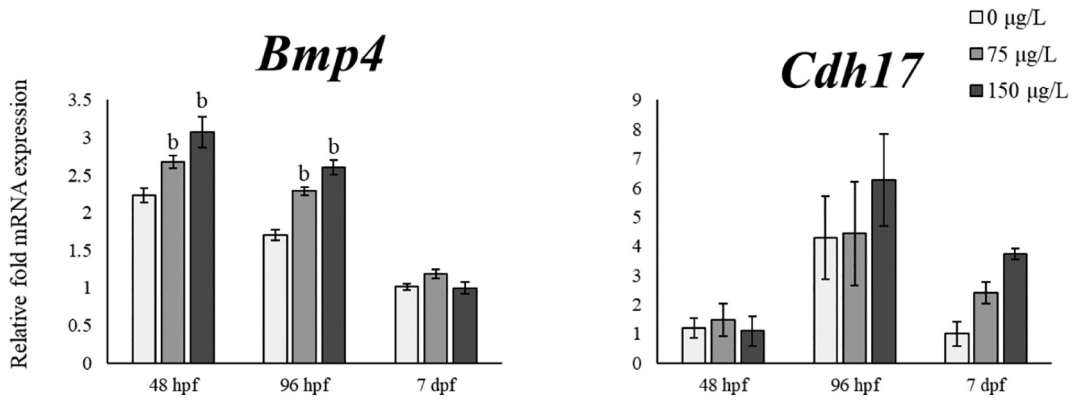

Fig. 4. Relative whole-body mRNA expression level of transcripts involved in general pronephros development and function. Transcripts were analyzed in zebrafish during HEWAF exposure (48 and 96 hpf) and after 3 days of recovery in clean control media (7 dpf). n = 6 (20 embryos/ larvae each) run in duplicate for 48 and 96 hpf; n = 6 (10 larvae each) run in duplicate for 0 and 75 µg/L ΣPAH at 7 dpf, and n = 3 for 150 µg/L ΣPAH at 7 dpf. Error bars represent ± SEM. Differences were considered significant at $P < 0.05$ (a = statistically different than control; b = statistically different than control and other treatment).

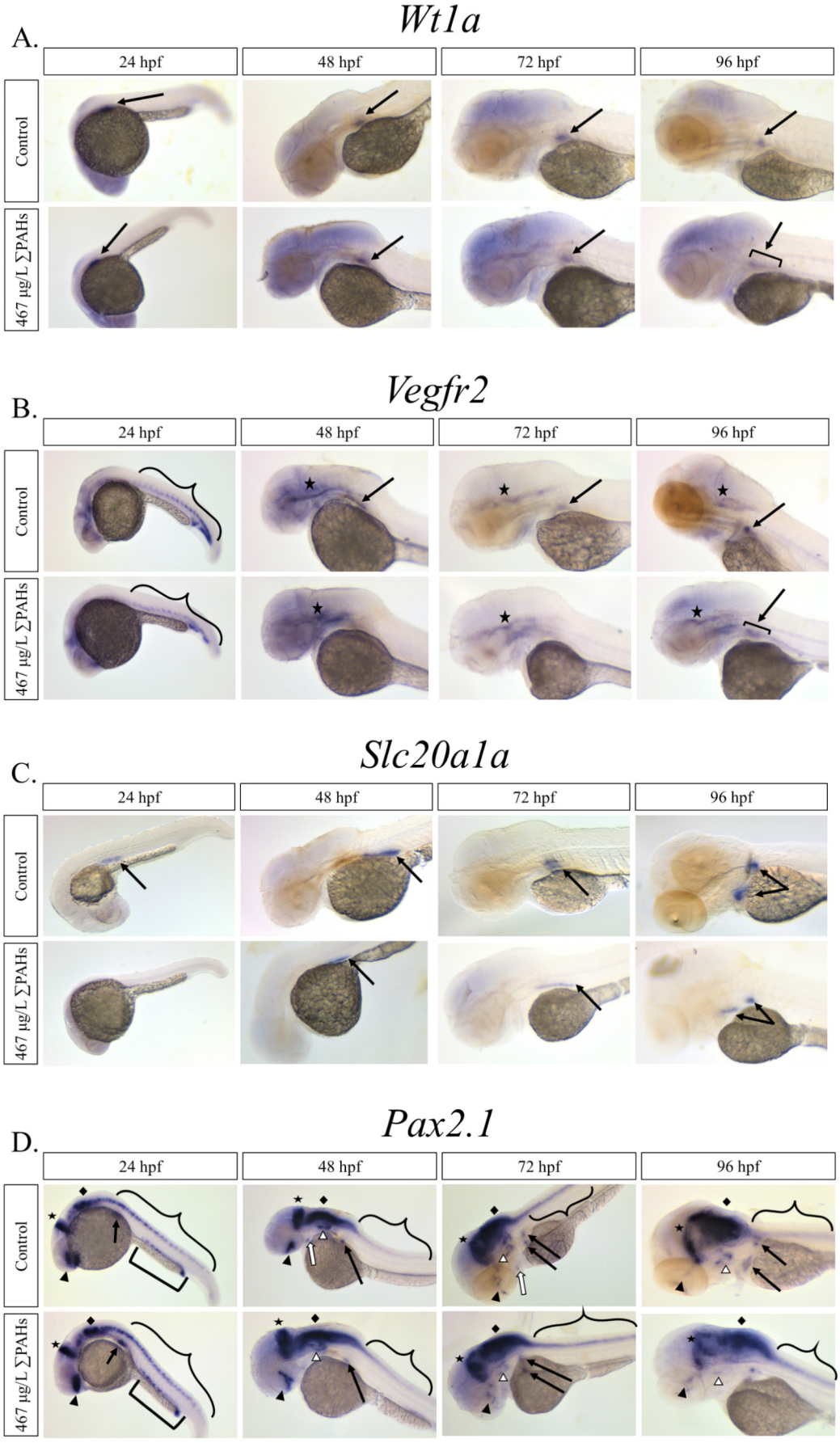
A.
Wt1a
24 hpf
48 hpf
72 hpf
96 hpf
Control
467 µg/L ∑PAHs
B.
Vegfr2
24 hpf
48 hpf
72 hpf
96 hpf
Control
467 µg/L ∑PAHs
C.
Slc20a1a
24 hpf
48 hpf
72 hpf
96 hpf
Control
467 µg/L ∑PAHs
D.
Pax2.1
24 hpf
48 hpf
72 hpf
96 hpf
Control
467 µg/L ∑PAHs

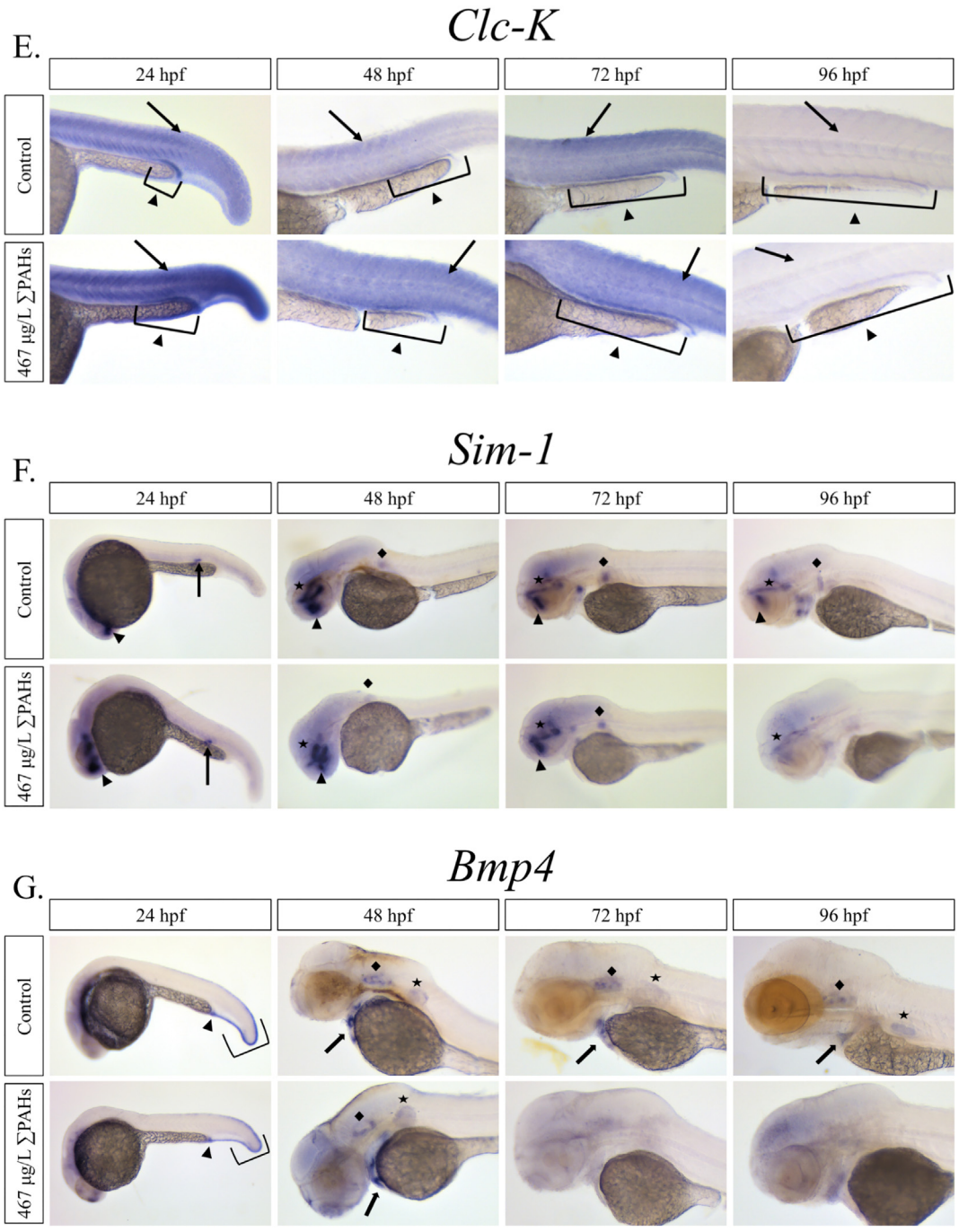

Fig. 5. Whole-mount in situ hybridization (WM-ISH) of various transcripts involved in pronephros development analyzed at 24, 48, 72 and 96 hpf in control zebrafish and zebrafish exposed to 467 µg/L ΣPAH. (A) wt1a WM-ISH (arrow, glomerulus). (B) vegfr2 WM-ISH (arrow, glomerulus; star, cranial vasculature; curly bracket, trunk vasculature). (C) slc20a1a WM-ISH (arrow, proximal tubules). (D) pax2.1 WM-ISH (black arrow, neck segments; box bracket, distal late and duct; curly bracket, spinal cord neurons; star, midbrain-hindbrain boundary; rhombus, hindbrain neurons; black triangle, optic stalk and choroid fissure; white triangle, otic vesicles; white arrow, thyroid primordium). (E) clc-K WM-ISH (triangle and box bracket, distal late and pronephric duct; arrow, skeletal muscles). (F) sim-1 WM-ISH (arrow, pronephric duct; triangle, optic recesses; star, hypothalamus and posterior tuberculum; rhombus, pectoral fins). (G) bmp4 WM-ISH (triangle, cloaca; box bracket, axial fin fold; arrow, heart; rhombus, otic vesicles; star, swim bladder).

Negative controls (sense probes and omitting the DIG-labeled probes) revealed no staining in 96 hpf zebrafish, indicating specificity of the DIG-labeled anti-sense probes (Fig. S4).

3.4. Whole-mount immunohistochemistry

An antibody raised against the Na^+ K^+ ATPase alpha-1 subunit was applied to highlight the zebrafish pronephros morphology at 72 hpf (Fig. 6). Incardona et al. (2004) previously showed than PHN exposure induces pronephric morphological defects, characterized by straightening of the proximal tubule and thinning of the pronephric epithelium in 80 hpf zebrafish. Similar results were observed with this study with 72 hpf zebrafish exposed to 467 µg/L ΣPAH and 56 µM (9.98 mg/L) PHN (Fig. 6g and h, respectively). However, these morphological defects where not easily observable in 72 hpf zebrafish exposed to 234 µg/L ΣPAH (Fig. 6f).

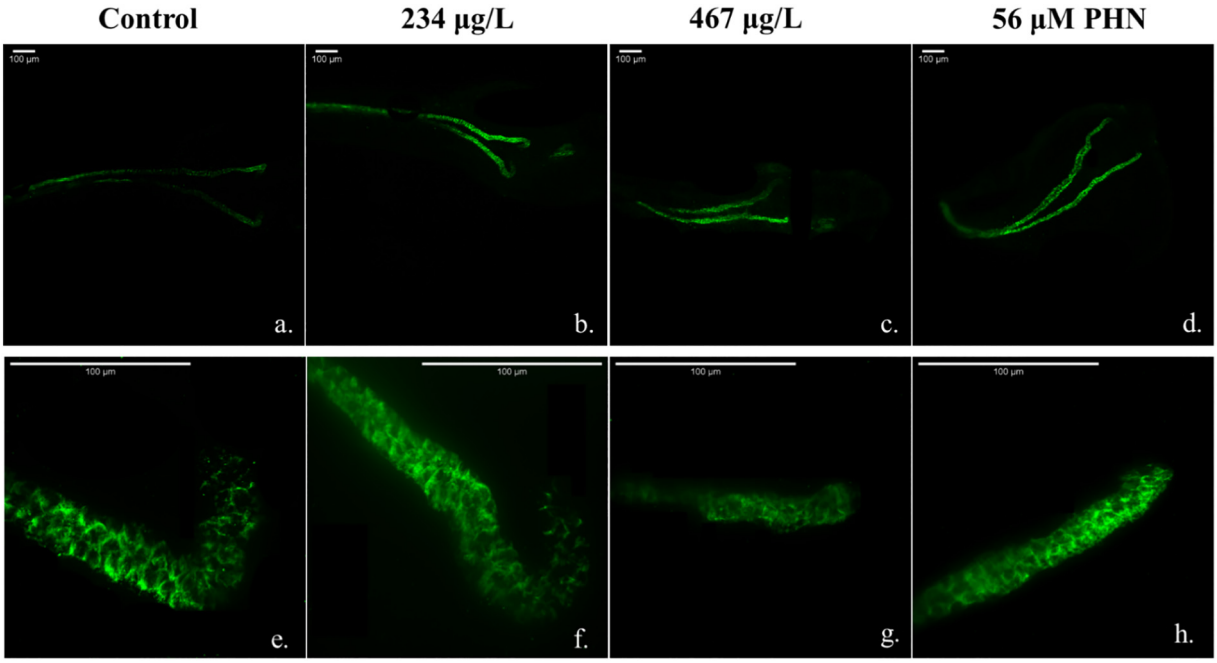

Fig. 6. Whole-mount immunohistochemistry (WM-IHC) performed with a monoclonal antibody against the Na^+/K^+ ATPase α-1 subunit in 72 hpf zebrafish larvae, highlighting the pronephric tubules and ducts. Fish were exposed to control water (a, e), 234 µg/ L ΣPAH (b,f), 467 µg/ L ΣPAH (c,g), and 56 µM phenanthrene (PHN) (d, f). Images were captured from a dorsal view of the whole pronephric tubules and duct (a-d) and subsequent recapture with higher magnification focusing on the proximal tubule (e-h; 2D projections of z-stacks of 23–29 optical sections).

3.5. 24 h osmotic challenge tests

Two different 24 h osmotic challenge tests, each using 3 different salinities, were performed post crude oil exposure: one initiated at 96 hpf (larvae from Test 1) and the other at 48 hpf (larvae from Test 2). Heart rate and pericardial and yolk-sac edema area were both quantified before and after the osmotic challenge.

With Test 1, after 96 h crude oil exposure (prior to the osmotic challenge), a significant increase in edema area and a significant decrease in heart rate were observed in a response fashion corresponding with the increase in PAH concentration (Fig. 7A and C, respectively). Edema and heart rate after the 24 h osmotic challenge test did not pass normality and equal variance tests even after exhausting all transformation possibilities. Nevertheless, a clear trend of increased edema was evident in larvae previously exposed to crude oil independent of water osmolarity (Fig. 7B). Moreover, an apparent concentration-response trend toward increasing bradycardia was observed in zebrafish previously exposed to crude oil (Fig. 7D). Although the trends observed for edema and heart rate were not statistically significant, these findings were consistent with previous studies of both marine and freshwater ELS fish exposed to crude oil (Grosell and Pasparakis, 2021; Incardona and Scholz, 2016).

Assessing edema size in Test 2, 48 hpf larvae previously exposed to crude oil showed little to no edema formation prior to the salinity challenge (Fig. 8A). However, edema was clearly visible in larvae previously exposed to crude oil following the 24 h osmotic challenge in clean waters (Fig. 8B). A concentration-response was observed in 72 hpf larvae challenged in Milli-Q water, with an increase in edema size corresponding with an increase in PAH concentration. Although not in a concentration-response fashion, a significant increase in edema size was also present in previously exposed fish when challenged in E3 medium (control water for the osmotic test). Despite the presence of pericardial edema in oil exposed fish challenged at lower salinities, there was no difference in pericardial area compared to control fish when challenged at near iso-osmotic conditions (25× NaCl E3 medium). This appeared to be due to a mild increase in pericardial area in control fish and a decrease in edema in fish that were previously exposed to 467 µg/L ΣPAH (both statistically different than fish challenged in Milli-Q water only).

Heart rate for 48 hpf zebrafish was not quantified due to a video quality issue. However, a reduction in heart rate was observed in zebrafish larvae that were previously exposed to crude oil at the end of the osmotic challenge (Fig. 8C). A concentration-response was observed in 72 hpf larvae challenged in Milli-Q water and in 25× NaCl E3 medium, with a decrease in heart rate corresponding with an increase in PAH concentration. Similarly, a significant reduction in heart rate was also present in previously exposed fish when challenged in E3 medium, but not in a concentration-response fashion. Furthermore, fish not previously exposed to crude oil, showed a significant increase in heart rate after the osmotic challenge in 25× NaCl E3 medium compared to Milli-Q water only. However, zebrafish that were previously exposed to 467 µg/L ΣPAH showed a significant decrease in heart rate after the osmotic challenge in 25× NaCl E3 medium compared to Milli-Q water only.

4. Discussion

With this study, we have shown that DWH crude oil ELS exposure induced molecular and morphological defects in the zebrafish pronephros. Moreover, post-exposure recovery in clean waters ranging in osmolarity from highly dilute (i.e., hypo-osmotic) to near iso-osmotic conditions revealed clear oil-induced impairments to maintaining proper fluid balance in ELS larvae. This was evidenced by increased pericardial and yolk sac edema, pointing to likely functional consequences in pronephros development associated with the observed molecular and morphological defects reported herein. Such defects might have arisen indirectly from downstream effects on the developing heart or via direct effects on the developmental programing of the pronephros. Considering the zebrafish heart begins beating at ~24 hpf (Burggren et al., 2017), and the role that the heart plays in pronephros development via hemodynamic forces (Serluca et al., 2002), it seems likely that impaired cardiac function played a significant role. However, mild alterations in the mRNA expression of select genes related to early pronephros development by WM-ISH at 24 hpf (i.e., around the

onset of heart contractions) hint at potential direct effects on pronephros development independent of cardiac function.

The gene transcripts targeted in this study were selected based on their known roles in the early development and function of specific pronephric regions, namely the glomerulus, neck segments, pronephric tubules and ducts. Development of the pronephric glomerulus appeared to be significantly altered in crude oil exposed zebrafish. This was apparent by *wt1a* and *vegfr2* WM-ISH analysis (Fig. 5A and B, respectively) where the expression of these two transcripts in the glomerulus failed to locate within their usual distinct locations. This was strongly evident for *vegfr2*, where its expression in the glomerulus was not observed in crude oil exposed fish starting at 48 hpf. Similarly, a non-specific and diffusive *wt1a* expression was observed in 96 hpf zebrafish exposed to crude oil suggesting impaired glomerulogenesis and morphological defects associated with the pronephric glomerulus. Similar observations were previously made in zebrafish with altered expression of *mmp-2* and *bmp4* (Serluca et al., 2002; Weber et al., 2008). Specifically, pharmacological inhibition of mmp-2 activity by the injection of tissue inhibitor of metalloproteinase-2 (TIMP-2) prevented proper glomerular formation in developing zebrafish larvae (Serluca et al., 2002); while morpholino knockdown of *bmp4* in zebrafish prevented the merging and fusion of the glomerulus, which was then characterized as a "large diffuse and unorganized aggregate" (Weber et al., 2008). Furthermore, a significant decrease in podocin mRNA expression (Fig. 2) was observed in zebrafish exposed to 150 μg/L ΣPAH at 48 hpf, a crucial timepoint for glomerular assembly (Drummond, 2003). Podocin is a structural protein expressed in the podocytes and is important for podocyte cell structure and the formation of the filtration barrier of the glomerulus (Kramer-Zucker et al., 2005b), which occurs at around 48 hpf. Inhibition of podocin expression previously resulted in failed slit-diaphragm formation and therefore failure to form a filtration apparatus in the pronephric glomerulus (Kramer-Zucker et al., 2005b). Taken together, these findings suggest that crude oil exposure likely elicits adverse effects on glomerulogenesis in the developing zebrafish.

By contrast, the analyses of additional transcripts related to the glomerulus revealed an increase in mRNA expression. Specifically, *wt1a* significantly increased in expression in fish exposed to 150 μg/L ΣPAH at 96 hpf, and *vegfr2* increased in exposed fish at 48 and 96 hpf (Figs. 2 and 1, respectively). Notably, overexpression of wt1s has been previously observed in isolated kidney tissue of adult killifish (*Aphaniops hormuzensis*) treated intra-peritoneally with 10 μg/g gentamicin, a known nephrotoxicant, at 5 days post injection (Motamedi et al., 2020). This molecular defect has been attributed to the lasting nephrotoxicity which resulted in the formation of numerous nephric cysts and the presence of detached epithelial cells in the tubules (Motamedi et al., 2020). Similarly, high expression of both *vegf* and *vegfr2* have been observed in kidneys affected by polycystic kidney disease (Tao et al., 2007), as well as in developing tumors (Ding et al., 2006; Eskens and Verweij, 2006). Although the presence of cysts was not assessed during our study, bilateral pronephric cysts were present in 80 hpf zebrafish exposed to PHN in a previous study (Incardona et al., 2004), suggesting that the increased expression of these two transcripts during the 96 h crude oil exposure might be related to cyst formation, although further confirmation is necessary.

Following the 3 days of recovery in clean water, zebrafish exposed to 150 μg/L ΣPAH exhibited increased expression of only transcripts believed to be involved in glomerulogenesis, which include *wt1b*, *vegf* (Drummond, 2003) and *mmp-9* (Serluca et al., 2002) (Figs. 2 and 1, respectively). It is important to mention that these transcripts, although vital for pronephros development, are not singularly involved in nephrogenesis, and thus might be involved in other pathways (Li et al., 2000; Scholz and Kirschner, 2011; Lo et al., 2014). The reason behind the observed overexpression of these transcripts in crude oil exposed zebrafish is unclear; however, overexpression has been previously observed during hypoxic conditions (Hendon et al., 2008; Scholz and Kirschner, 2011; Evans et al., 2012) and during tumor formation (Ding et al., 2006; Scholz and Kirschner, 2011). In response to hypoxic conditions, the aryl hydrocarbon receptor nuclear translocators (ARNTs) can form dimer complexes with the hypoxia inducible factors (HIFs) and upregulate the expression of hypoxia-induced genes (Hendon et al., 2008; Hill et al., 2009). Interestingly, reduction in cardiac output in developing fish may result in hypoxic signaling activation, as has been observed in breakdance mutant zebrafish larvae (characterized by reduced cardiac output) starting at 72 hpf by the increased expression of both *HIF-1α* and *vegf* (Kopp et al., 2010). Therefore, the observed and well-known crude oil induced cardiotoxicity may contribute to the activation of hypoxic signaling in the exposed larvae. Additionally, crude oil and PAHs can induce toxicity via the aryl hydrocarbon receptor (AhR) pathway (Grosell and Pasparakis, 2021), which also involves the ARNT. Given that both AhR and hypoxia signaling pathways require interaction with ARNT, a cross-talk between these two pathways has been proposed (Nie et al., 2001; Vorrink and Domann, 2014), however supporting information remains scarce. Cross-talk has also been investigated with the pathway involving *sim-1*, as it also belongs to the PAS family of transcription factors and dimerizes with ARNT (Yang et al., 2004; Hill et al., 2009), potentially explaining the differences in *sim-1* mRNA level in crude oil exposed zebrafish. Investigating further into the interaction between these pathways could provide significant insight into crude oil toxicity. Furthermore, the increased expression of these transcripts due to the development of cysts and/or tumors cannot be ruled out given the carcinogenic nature of PAHs (Ding et al., 2006) and the previously observed cysts in exposed fish (Incardona et al., 2004).

The significant spike in *mmp-9* expression after the 3 days of recovery was somewhat surprising (Fig. 1). In addition to what was previously discussed, MMPs are also involved in angiogenic processes, specifically in the remodeling of the vasculature basement membrane and extracellular matrix (Li et al., 2000), which are necessary to promote the formation of new vessels. Particularly, *mmp-9* function has been associated with the maintenance of the basement membrane around the cardiomyocytes (Zhang et al., 2013). In fact, zebrafish larvae exposed to PHN showed an increased expression and activity of MMP-9 in addition to cardiotoxic defects (ventricle dilation, wall thinning, and overall cardiac disfunction), a phenotype that was rescued with the dosage of MMP-9 inhibitor (Zhang et al., 2013). This evidence further suggests the significant implications of crude oil exposure related to the cardiovascular system in teleost fish; however, it is unclear why no differences associated with MMP transcript expression were observed during the 96 h exposure. Nevertheless, potential cardiotoxic effects at the molecular level might be associated with the concentration-response increase in expression of *bmp4* mRNA during the crude oil exposure (Fig. 4), as previous studies have associated altered expression of this transcript with developmental cardiac defects (Li et al., 2020) and cardiotoxicity (Huang et al., 2018). This was further confirmed by WM-ISH analysis in the present study, which revealed altered *bmp4* mRNA expression (Fig. 5G) in oil exposed zebrafish at all time points examined, most notably starting at 72 hpf which showed failed or unspecified expression associated with the heart, otic vesicles, and swim bladder.

In addition to glomerulogenesis, pronephric neck segment development and morphology appeared to be altered by crude oil exposure in zebrafish, which was suggested by the *pax2.1* analysis. *Pax2.1* is a transcription factor expressed by the neck segments, and is an important marker for cell differentiation in the pronephros, as it is involved in restricting the expression domain of podocyte markers, such as *wt1* and *vegf* (Drummond et al., 1998; Outtandy et al., 2019). In support of this, the *pax2.1* no isthmus zebrafish mutant strain showed the expression of these glomerulus-specific genes (*wt1* and *vegf*) in the anterior proximal tubules, in addition to the absence of neck segments (Majumdar et al., 2000). By WM-ISH analysis, it was possible to observe that 96 hpf crude oil exposed zebrafish failed to properly form the neck segments (Fig. 5D), as it has been observed in the *pax2.1* no isthmus zebrafish previously mentioned. However, it is difficult to assess if the quantified difference in mRNA expression is related singularly to the pronephros, as *pax2.1* is highly expressed in other areas in the developing zebrafish, such as the hindbrain, spinal cord, thyroid primordium, otic vesicles, and eyes.

The different segments of the developing pronephric tubules and pronephric ducts are characterized by the expression of specific ion

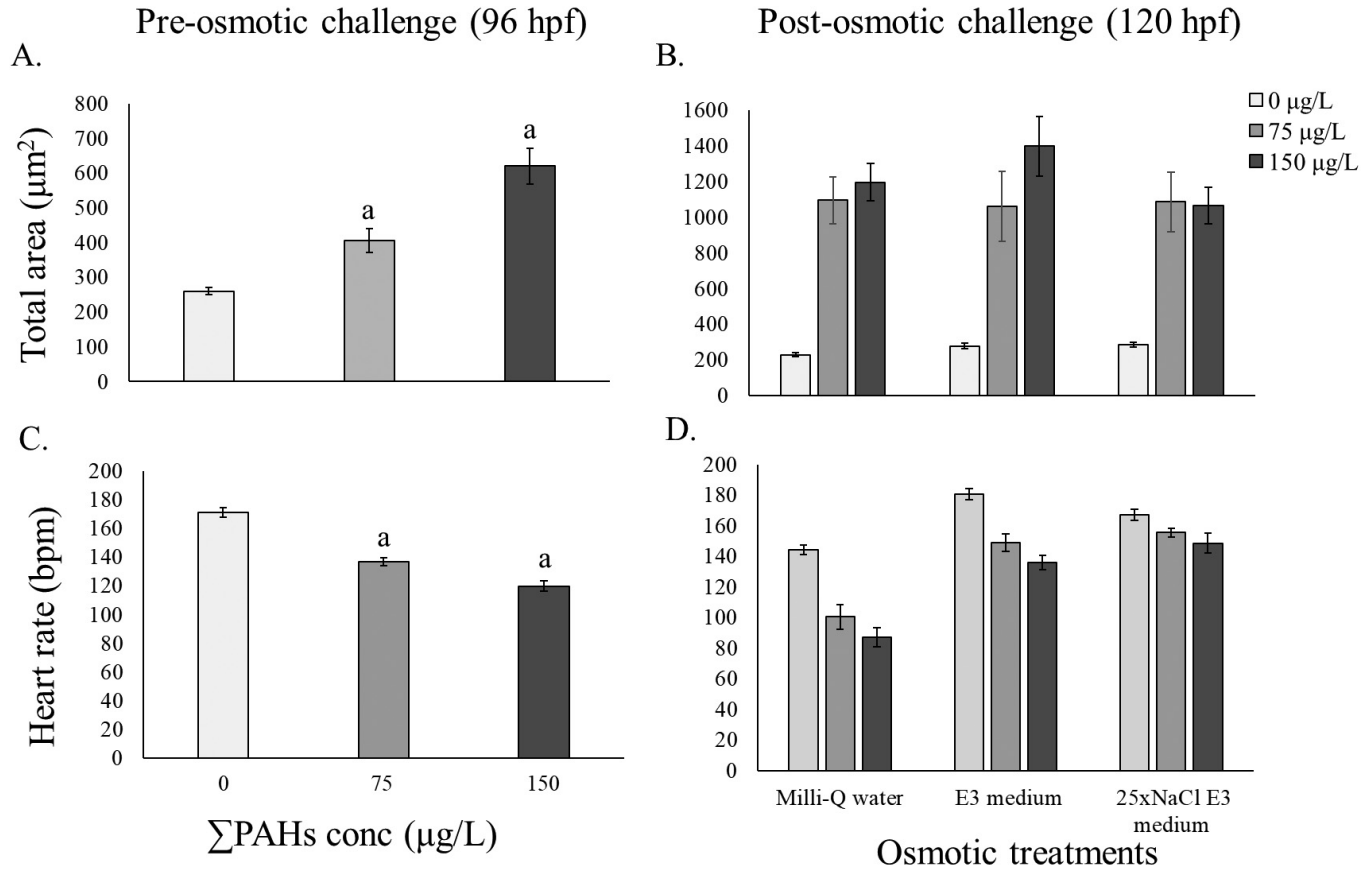

Fig. 7. Test 1 results related to edema size and heart rate pre- and post-osmotic challenge. (A) represents pericardial/ yolk-sac edema area right after 96-h HEWAF exposure and right before the 24 h osmotic challenge (zebrafish larvae at 96 hpf); (B) represents pericardial/yolk-sac edema area right after the 24 h osmotic challenge (zebrafish larvae at 120 hpf); (C) represents heart rate, measured in beats per minutes (bpm), right after 96 h HEWAF exposure and right before the 24 h osmotic challenge (zebrafish larvae at 96 hpf); (D) represents heart rate, measured in bpm, right after the 24 h osmotic challenge (zebrafish larvae at 120 hpf). Error bars represent ± SEM (n = 13–16). Differences were considered significant at $P < 0.05$ (a = statistically different than control; b = statistically different than control and other HEWAF treatment). Edema area and heart rate after the 24 h osmotic challenge test did not pass normality and equal variance.

transporters and channels (Wingert et al., 2007). Some of these functional proteins are solute carrier family 20 member 1 (*slc20a1a*) in the proximal convoluted tubule (PCT), and chloride channel K (*clcK*) in the distal late (DL) and pronephric duct. They are both expressed from 24 hpf in the developing zebrafish and potentially already play a role in osmoregulation (Kersten and Arjona, 2016). *Slc20a1a* is associated with a sodium-dependent phosphate transporter, and it is usually targeted in studies to easily observe morphological changes in the PCT segment during development (McCampbell and Wingert, 2014). On the other hand, *clc-K* plays an important role in chloride osmoregulation within zebrafish larvae, as knockout of *clc-K* reduces chloride concentration in 7 dpf larvae, which then results in mortality at 10 dpf (Pérez-Rius et al., 2019). Interestingly, the expression of both *slc20a1a* and *clc-K* mRNA was increased in crude oil exposed zebrafish at 96 hpf (Fig. 3). This observation might suggest the presence of altered internal ion homeostasis due to potential crude oil effects on osmoregulation and acid/base balance (Grosell and Pasparakis, 2021), which could further play a role in edema formation. Notably, our result showed that only 96 hpf zebrafish exposed to the lowest HEWAF dilution expressed an increase in *slc20a1a* mRNA level, potentially indicating that higher ΣPAH concentration might have induced an insult too severe to initiate the response. Furthermore, analysis by WM-ISH demonstrated that *slc20a1a* is singularly expressed on the proximal tubule (Fig. 5C), and that crude oil and PHN exposed zebrafish have an altered morphology of the PCT, as evidenced by being thinner and exhibiting a straight instead of a convoluted shape (Fig. 6). Similar morphological defects were previously observed in 80 hpf zebrafish exposed to PHN (Incardona et al., 2004), and in zebrafish exposed to benzo(*a*)pyrene, another PAH present in crude oil, in addition to failed glomerulus formation (Lo et al., 2014). Additionally, both *slc20a1a* and *clc-K* expression, analyzed by WM-ISH, was altered in crude oil exposure at 24 hpf, characterized by an indistinctive expression in the pronephric tubules (Fig. 5C) and elongated expression in the pronephric ducts (Fig. 5E), respectively. Importantly, these molecular defects might represent direct effects on the specification of early nephric segments given the timing of occurrence, which is around the onset of coordinated heart contractions (Burggren et al., 2017).

Failure in proper pronephros development most likely results in functional defects (Kramer-Zucker et al., 2005b; Perner et al., 2007). While the integument of ELS fishes plays a role in water and ion regulation at first, the developing kidney seems to play an important role in water excretion relatively early, especially in freshwater larvae (Hentschel et al., 2007; Rider et al., 2012). Therefore, given the importance of the pronephros clearance capacity during ELS fish development, any factors affecting the excretory ability of the pronephros could result in liquid accumulation in fish larvae. Specific to zebrafish larvae, while gills do not become functional until 7 dpf, a functional pronephros is observed between 40 and 48 hpf, which is characterized by the onset of glomerular filtration (Drummond, 2003). Notably, failure in zebrafish pronephros development and/or function, induces the presence of pericardial and yolk-sac edema at ~72 hpf and a more general edema at 120 hpf (Kramer-Zucker et al., 2005b; Perner et al., 2007), which is a sign of impaired water balance/excretion and osmoregulation in general. It is important to point out that the zebrafish is a freshwater species, and as such its pronephros plays a different osmoregulatory role compared to the pronephros of fishes that inhabit hyper-osmotic salt-waters. Freshwater species use their kidney to excrete a

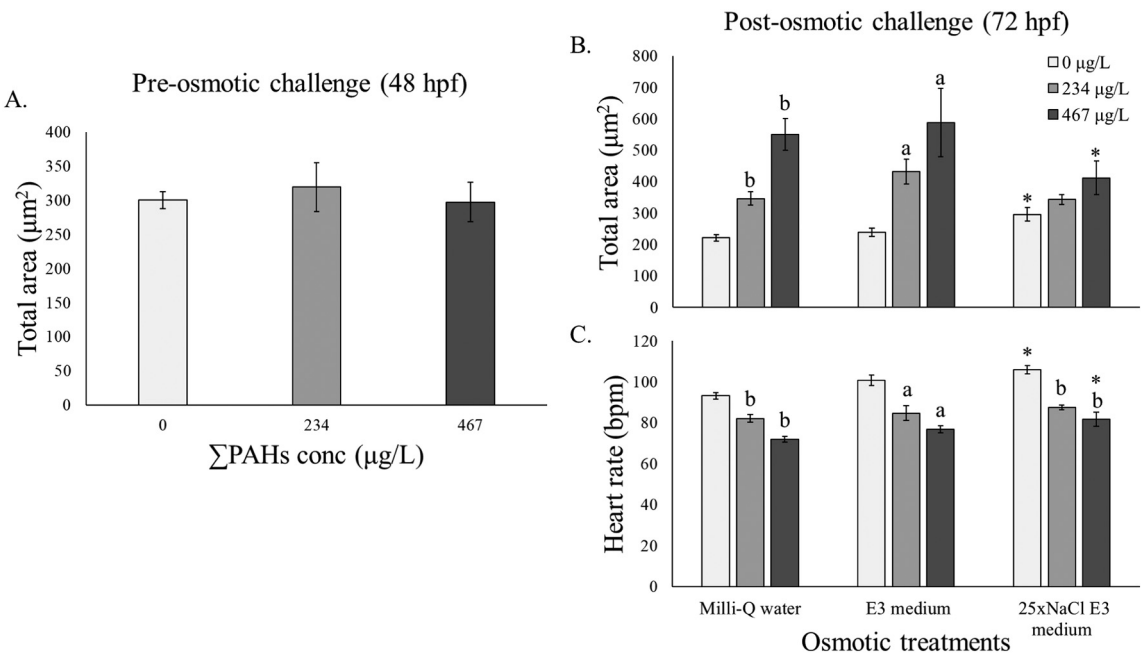

Fig. 8. Test 2 results related to edema size and heart rate pre- and post-osmotic challenge. (A) represents pericardial/ yolk-sac edema area size right after 48 h HEWAF exposure and right before the 24 h osmotic challenge (zebrafish larvae at 48 hpf); (B) represents pericardial/ yolk-sac edema area size right after the 24 h osmotic challenge (zebrafish larvae at 72 hpf); (C) represents heart rate, measured in beats per minutes (bpm), right after the 24 h osmotic challenge (zebrafish larvae at 72 hpf). Error bars represent ± SEM (n = 9–10). Differences were considered significant at $P < 0.05$ (a = statistically different than control; b = statistically different than control and other HEWAF treatment; * = statistically different than fish challenged in Milli-Q water within the same HEWAF treatment).

high amount of dilute urine to eliminate excess water gained by passive diffusion, while saltwater fish excrete a small amount of concentrated urine to conserve water. Yet, renal clearance capacity appears to develop relatively early in fish that inhabit fresh- (Kramer-Zucker et al., 2005a; Rider et al., 2012) and/or salt-waters (Tytler et al., 1996; Tytler and Ireland, 2000; Fedorova et al., 2008; Abadi et al., 2014), not only for osmoregulatory purposes, but mostly for proper pronephros development (Kramer-Zucker et al., 2005a; Freund et al., 2012), as fluid flow within the pronephros is required for collective cell migration and nephric segmentation.

Not surprisingly, after a 96 h exposure to 0, 75 and 150 µg/L ΣPAH (exposure ending at 96 hpf) a significant increase in edema size (Fig. 7A) and a significant decrease in heart rate (Fig. 7C) was observed in a concentration-response fashion with an increase in ΣPAH concentration. These observations corroborate the crude oil induced cardiotoxicity and edema previously reported in other studies (Incardona et al., 2004; Incardona and Scholz, 2016; Magnuson et al., 2020). While a lack of equal variance and normality precluded statistical comparisons, the data presented in Fig. 7B clearly reveals a likely detrimental effect of crude oil exposure on the osmoregulatory ability of ELS zebrafish. A similar analysis was performed following the 24 h osmotic challenge, but no effects of different water osmolarity and/or ΣPAH concentration were observed, as crude oil exposed zebrafish (now 120 hpf) presented an enlarged edema throughout the whole-body, which appeared likely irreversible and "maxed out" in size (Fig. 7B). This result suggests that the insult induced by crude oil exposure was too severe to observe a concentration-response at the concentrations used, but most importantly that water excretion was highly reduced or completely negated. Nevertheless, the observed phenotype resembles that of zebrafish larvae with altered pronephros development and characterized by a pericardial edema at 72 hpf and a more general edema at 120 hpf as previously described by Kramer-Zucker et al. (2005b) and Perner et al. (2007). This phenotypic similarity suggests that the molecular and morphological pronephric defects induced by crude oil exposure are playing a role in the induced edema formation and expansion, as the larvae might not be able to excrete water efficiently through the pronephros. However, renal clearance capacity in oil exposed fish needs to be tested to confirm this hypothesis. Additionally, cardiotoxicity was confirmed as heart rate appeared to be reduced in zebrafish larvae previously exposed to crude oil (Fig. 7D).

A second osmotic challenge test was then performed at an earlier time point to enhance the chances of observing a concentration-response in edema size, which was not observed with the previous test, likely due to the severity of the insult. Interestingly, edema was not present after 48 h HEWAF exposure (Fig. 8A); however, after the osmotic challenge test, a concentration-response in edema area was, in fact, observed (Fig. 8B). These observations strongly suggest the importance of pronephric function in water excretion and therefore crude oil induced edema formation, which occurs after the supposed onset of glomerular ultrafiltration (48 hpf) but not prior (Drummond, 2003). To further characterize the observed edema after the 24 h osmotic challenge (zebrafish now at 72 hpf) (Fig. 8B), previously crude oil exposed larvae that were challenged in hypo-osmotic waters (Milli-Q water and E3 medium) revealed a significant increase in edema. However, challenging zebrafish larvae to water near iso-osmotic conditions neutralized the differences in pericardial/yolk sac edema size between control fish and previously crude oil exposed fish. All combined, the concentration-response observed in edema size in fish challenged in extreme hypo-osmotic water (Milli-Q water) tended to be negated with an increase in water osmolarity. Aside from edema, cardiotoxicity was confirmed by a reduction in heart rate in crude oil exposed fish (Fig. 8C), similar to the previously discussed osmotic challenge test. In fact, heart rate was reduced independently of the different water osmolarities.

5. Conclusion

Crude oil toxicity has been widely studied during the past decades. However, this is the first comprehensive study that has specifically focused on the toxic effects of crude oil exposure during ELS to the developing teleost kidney. Overall, differences in mRNA expression of kidney specific genes were observed at 48 and 96 hpf in exposed zebrafish, which likely led to developmental and morphological defects associated with the pronephros. Some of the transcripts examined are also involved in other, non-kidney specific pathways that,

through further investigation might provide additional information regarding crude oil toxicity in developing fish. Furthermore, by WM-ISH analysis it was confirmed that other tissues are influenced by crude oil exposure in addition to the pronephros, such as the heart, eyes, and otic vesicles. Given the importance of fluid flow within the kidney and the obligatory fluid clearance (Hentschel et al., 2005; Gerlach and Wingert, 2013), the inability to excrete fluid through the ELS pronephros can potentially result in water accumulation, or edema, regardless of living in a freshwater or saltwater environment. Therefore, the observed molecular and morphological defects during pronephros development likely have important implications in osmoregulation and edema formation in crude oil exposed fish. However, these remain speculations as more complex mechanisms can be involved and therefore warrant additional study. Given the heart plays a major role in fluid flow and excretion through the pronephros in ELS fish, the reduced cardiac output commonly associated with crude oil exposure likely plays an integral role in the observed effects on pronephros development and renal clearance capacity.

CRediT authorship contribution statement

Fabrizio Bonatesta: Conceptualization, Methodology, Formal analysis, Investigation, Data curation, Writing – original draft, Writing – review & editing, Visualization. **Cameron Emadi:** Investigation, Writing – review & editing. **Edwin R. Price:** Investigation, Writing – review & editing. **Yadong Wang:** Methodology, Resources, Writing – review & editing. **Justin Greer:** Methodology, Resources, Writing – review & editing. **Elvis Genbo Xu:** Methodology, Resources, Writing – review & editing. **Daniel Schlenk:** Methodology, Resources, Writing – review & editing, Funding acquisition. **Martin Grosell:** Methodology, Resources, Writing – review & editing, Funding acquisition. **Edward M. Mager:** Conceptualization, Methodology, Resources, Writing – original draft, Writing – review & editing, Supervision, Project administration, Funding acquisition.

Declaration of competing interest

The authors declare that they have no known competing financial interests or personal relationships that could have appeared to influence the work reported in this paper.

Acknowledgments

This work was supported by the Gulf of Mexico Research Initiative [Grant No. SA-1520 to the RECOVER consortium (Relationship of effects of cardiac outcomes in fish for validation of ecological risk)], the Cristina and Charles Johnson Foundation, and University of North Texas start-up funds. JG was supported in part by the U.S. Geological Survey's (USGS) Environmental Health Program (Contaminant Biology and Substances Hydrology). MG is a Maytag Professor of Ichthyology. We thank Dr. Andrea Bernardino from the University of North Texas for the assistance and consultation with the confocal microscope operation. We also thank the three anonymous reviewers for their valuable feedback and helpful suggestions for improving the manuscript. Data are publicly available through the Gulf of Mexico Research Initiative Information and Data Cooperative (GRIIDC), at https://data.gulfresearchinitiative.org (doi: https://doi.org/10.7266/BFXBPAD8; and doi: https://doi.org/10.7266/P5GD67N3). Any use of trade, firm, or product names is for descriptive purposes only and does not imply endorsement by the U.S. Government.

Appendix A. Supplementary data

Supplementary data to this article can be found online at https://doi.org/10.1016/j.scitotenv.2021.151988.

References

Abadi, Z.T.R., Khodabandeh, S., Charmantier, G., Charmantier-Daures, M., Lignot, J.H., 2014. Ontogeny and osmoregulatory function of the urinary system in the Persian sturgeon, Acipenser persicus (Borodin, 1897). Tissue Cell 46 (5), 287–298. https://doi.org/10.1016/j.tice.2014.02.003.

Bai, W., Zhang, Z., Tian, W., He, X., Ma, Y., Zhao, Y., Chai, Z., 2010. Toxicity of zinc oxide nanoparticles to zebrafish embryo: a physicochemical study of toxicity mechanism. J. Nanopart. Res. 12 (5), 1645–1654. https://doi.org/10.1007/s11051-009-9740-9.

Burggren, W.W., Dubansky, B., Bautista, N.M., 2017. 2 - cardiovascular development in embryonic and larval fishes. (The Cardiovascular System)In: Gamperl, A.K., Gillis, T.E., Farrell, A.P., Brauner, C.J. (Eds.), Fish Physiology. vol. 36. Academic Press , pp. 107–184. http://www.sciencedirect.com/science/article/pii/S1546509817300274. (Accessed 31 August 2020).

Dent, J.A., Polson, A.G., Klymkowsky, M.W., 1989. A whole-mount immunocytochemical analysis of the expression of the intermediate filament protein vimentin in Xenopus. Development 105 (1), 61–74.

Ding, J., Li, J., Chen, J., Chen, H., Ouyang, W., Zhang, R., Xue, C., Zhang, D., Amin, S., Desai, D., et al., 2006. Effects of polycyclic aromatic hydrocarbons (PAHs) on vascular endothelial growth factor induction through phosphatidylinositol 3-kinase/AP-1-dependent, HIF-1α-independent pathway. J. Biol. Chem. 281 (14), 9093–9100. https://doi.org/10.1074/jbc.M510537200.

Drummond, I., 2003. Making a zebrafish kidney: a tale of two tubes. Trends Cell Biol. 13 (7), 357–365. https://doi.org/10.1016/S0962-8924(03)00124-7.

Drummond, I.A., 2005. Kidney development and disease in the zebrafish. J. Am. Soc. Nephrol. 16 (2), 299–304. https://doi.org/10.1681/ASN.2004090754.

Drummond, I.A., Majumdar, A., Hentschel, H., Elger, M., Solnica-Krezel, L., Schier, A.F., Neuhauss, S.C., Stemple, D.L., Zwartkruis, F., Rangini, Z., et al., 1998. Early development of the zebrafish pronephros and analysis of mutations affecting pronephric function. Development 125 (23), 4655–4667.

Eckle, P., Burgherr, P., Michaux, E., 2012. Risk of large oil spills: a statistical analysis in the aftermath of Deepwater Horizon. Environ. Sci. Technol. 46 (23), 13002–13008. https://doi.org/10.1021/es3029523.

Edmunds, R.C., Gill, J.A., Baldwin, D.H., Linbo, T.L., French, B.L., Brown, T.L., Esbaugh, A.J., Mager, E.M., Stieglitz, J., Hoenig, R., et al., 2015. Corresponding morphological and molecular indicators of crude oil toxicity to the developing hearts of mahi mahi. Sci. Rep. 5 (1), 17326. https://doi.org/10.1038/srep17326.

Esbaugh, A.J., Mager, E.M., Stieglitz, J.D., Hoenig, R., Brown, T.L., French, B.L., Linbo, T.L., Lay, C., Forth, H., Scholz, N.L., et al., 2016. The effects of weathering and chemical dispersion on Deepwater Horizon crude oil toxicity to mahi-mahi (Coryphaena hippurus) early life stages. Sci. Total Environ. 543, 644–651. https://doi.org/10.1016/j.scitotenv.2015.11.068.

Eskens, F.A.L.M., Verweij, J., 2006. The clinical toxicity profile of vascular endothelial growth factor (VEGF) and vascular endothelial growth factor receptor (VEGFR) targeting angiogenesis inhibitors.A review. Eur. J. Cancer 42 (18), 3127–3139. https://doi.org/10.1016/j.ejca.2006.09.015.

Evans, L.C., Liu, H., Pinkas, G.A., Thompson, L.P., 2012. Chronic hypoxia increases peroxynitrite, MMP9 expression, and collagen accumulation in fetal guinea pig hearts. Pediatr. Res. 71 (1), 25–31. https://doi.org/10.1038/pr.2011.10.

Fedorova, S., Miyamoto, R., Harada, T., Isogai, S., Hashimoto, H., Ozato, K., Wakamatsu, Y., 2008. Renal glomerulogenesis in medaka fish, Oryzias latipes. Dev. Dyn. 237 (9), 2342–2352. https://doi.org/10.1002/dvdy.21687.

Forth, H.P., Mitchelmore, C.L., Morris, J.M., Lipton, J., 2017. Characterization of oil and water accommodated fractions used to conduct aquatic toxicity testing in support of the Deepwater Horizon oil spill natural resource damage assessment. Environ. Toxicol. Chem. 36 (6), 1450–1459. https://doi.org/10.1002/etc.3672.

Freund, J.B., Goetz, J.G., Hill, K.L., Vermot, J., 2012. Fluid flows and forces in development: functions, features and biophysical principles. Development 139 (7), 1229–1245. https://doi.org/10.1242/dev.073593.

Gerlach, G.F., Wingert, R.A., 2013. Kidney organogenesis in the zebrafish: insights into vertebrate nephrogenesis and regeneration. Wiley Interdiscip. Rev. Dev. Biol. 2 (5), 559–585. https://doi.org/10.1002/wdev.92.

Grosell, M., Pasparakis, C., 2021. Physiological responses of fish to oil spills. Annu. Rev. Mar. Sci. 13 (1). https://doi.org/10.1146/annurev-marine-040120-094802 null.

Hendon, L.A., Carlson, E.A., Manning, S., Brouwer, M., 2008. Molecular and developmental effects of exposure to pyrene in the early life-stages of Cyprinodon variegatus. Comp. Biochem.Physiol. Part C Toxicol.Pharmacol. 147 (2), 205–215. https://doi.org/10.1016/j.cbpc.2007.09.011.

Hentschel, D.M., Park, K.M., Cilenti, L., Zervos, A.S., Drummond, I., Bonventre, J.V., 2005. Acute renal failure in zebrafish: a novel system to study a complex disease. Am.J.Physiol.Ren. Physiol. 288 (5), F923–F929. https://doi.org/10.1152/ajprenal.00386.2004.

Hentschel, D.M., Mengel, M., Boehme, L., Liebsch, F., Albertin, C., Bonventre, J.V., Haller, H., Schiffer, M., 2007. Rapid screening of glomerular slit diaphragm integrity in larval zebrafish. Am.J.Physiol.Ren. Physiol. 293 (5), F1746–F1750. https://doi.org/10.1152/ajprenal.00009.2007.

Hill, A.J., Heiden, T.C.K., Heideman, W., Peterson, R.E., 2009. Potential roles of Arnt2 in zebrafish larval development. Zebrafish 6 (1), 79–92.

Huang, M., Jiao, J., Wang, J., Xia, Z., Zhang, Y., 2018. Exposure to acrylamide induces cardiac developmental toxicity in zebrafish during cardiogenesis. Environ. Pollut. 234, 656–666. https://doi.org/10.1016/j.envpol.2017.11.095.

Incardona, J.P., Scholz, N.L., 2016. The influence of heart developmental anatomy on cardiotoxicity-based adverse outcome pathways in fish. Aquat. Toxicol. 177, 515–525. https://doi.org/10.1016/j.aquatox.2016.06.016.

Incardona, J.P., Collier, T.K., Scholz, N.L., 2004. Defects in cardiac function precede morphological abnormalities in fish embryos exposed to polycyclic aromatic hydrocarbons. Toxicol. Appl. Pharmacol. 196 (2), 191–205. https://doi.org/10.1016/j.taap.2003.11.026.

Incardona, J.P., Swarts, T.L., Edmunds, R.C., Linbo, T.L., Aquilina-Beck, A., Sloan, C.A., Gardner, L.D., Block, B.A., Scholz, N.L., 2013. Exxon Valdez to Deepwater Horizon: comparable toxicity of both crude oils to fish early life stages. Aquat. Toxicol. 142–143, 303–316. https://doi.org/10.1016/j.aquatox.2013.08.011.

Jung, J.-H., Hicken, C.E., Boyd, D., Anulacion, B.F., Carls, M.G., Shim, W.J., Incardona, J.P., 2013. Geologically distinct crude oils cause a common cardiotoxicity syndrome in developing zebrafish. Chemosphere 91 (8), 1146–1155. https://doi.org/10.1016/j.chemosphere.2013.01.019.

Kersten, S., Arjona, F.J., 2016. Ion transport in the zebrafish kidney from a human disease angle: possibilities, considerations, and future perspectives. Am.J.Physiol.Ren. Physiol. 312 (1), F172–F189. https://doi.org/10.1152/ajprenal.00425.2016.

Khursigara, A.J., Johansen, J.L., Esbaugh, A.J., 2018. Social competition in red drum (Sciaenops ocellatus) is influenced by crude oil exposure. Aquat. Toxicol. 203, 194–201. https://doi.org/10.1016/j.aquatox.2018.08.011.

Kopp, R., Schwerte, T., Egg, M., Sandbichler, A.M., Egger, B., Pelster, B., 2010. Chronic reduction in cardiac output induces hypoxic signaling in larval zebrafish even at a time when convective oxygen transport is not required. Physiol. Genomics 42A (1), 8–23. https://doi.org/10.1152/physiolgenomics.00052.2010.

Kozłowski, T.M., Jönsson, M., Ek, F., Olsson, R., Kröger, R.H.H., 2017. Osmotic concentration of zebrafish (Danio rerio) body fluids is lower in larvae than in adults. Zebrafish 15 (1), 9–14. https://doi.org/10.1089/zeb.2017.1504.

Kramer-Zucker, A.G., Olale, F., Haycraft, C.J., Yoder, B.K., Schier, A.F., Drummond, I.A., 2005. Cilia-driven fluid flow in the zebrafish pronephros, brain and Kupffer's vesicle is required for normal organogenesis. Development 132 (8), 1907–1921. https://doi.org/10.1242/dev.01772.

Kramer-Zucker, A.G., Wiessner, S., Jensen, A.M., Drummond, I.A., 2005. Organization of the pronephric filtration apparatus in zebrafish requires nephrin, podocin and the FERM domain protein Mosaic eyes. Dev. Biol. 285 (2), 316–329. https://doi.org/10.1016/j.ydbio.2005.06.038.

Larsen, E.H., Deaton, L.E., Onken, H., O'Donnell, M., Grosell, M., Dantzler, W.H., Weihrauch, D., 2014. Osmoregulation and excretion. Comprehensive Physiology. American Cancer Society , pp. 405–573. https://onlinelibrary.wiley.com/doi/abs/10.1002/cphy.c130004. (Accessed 31 August 2020).

Li, Y.Y., McTiernan, C.F., Feldman, A.M., 2000. Interplay of matrix metalloproteinases, tissue inhibitors of metalloproteinases and their regulators in cardiac matrix remodeling. Cardiovasc. Res. 46 (2), 214–224. https://doi.org/10.1016/s0008-6363(00)00003-1.

Li, X., Xiong, D., Ding, G., Fan, Y., Ma, X., Wang, C., Xiong, Y., Jiang, X., 2019. Exposure to water-accommodated fractions of two different crude oils alters morphology, cardiac function and swim bladder development in early-life stages of zebrafish. Chemosphere 235, 423–433. https://doi.org/10.1016/j.chemosphere.2019.06.199.

Li, B., Chen, J., Du, Q., Wang, B., Qu, Y., Chang, Z., 2020. Toxic effects of dechlorane plus on the common carp (Cyprinus carpio) embryonic development. Chemosphere 249, 126481. https://doi.org/10.1016/j.chemosphere.2020.126481.

Li, X., Xiong, D., Ju, Z., Xiong, Y., Ding, G., Liao, G., 2021. Phenotypic and transcriptomic consequences in zebrafish early-life stages following exposure to crude oil and chemical dispersant at sublethal concentrations. Sci. Total Environ. 763, 143053. https://doi.org/10.1016/j.scitotenv.2020.143053.

Lo, K.-C., Sun, C.-Y., Ding, Y.-J., Tsai, J.-N., Chang, K.-P., Wen, Y.-E., Chang, W.-L., Chang, S.C., Chang, M.-F., Wang, Y.-H., et al., 2014. Nephrotoxicity assessments of benzo(a)pyrene during zebrafish embryogenesis. Res. Chem. Intermed. 40 (6), 2177–2185. https://doi.org/10.1007/s11164-014-1595-8.

Ma, M., Jiang, Y.-J., 2007. Jagged2a-Notch signaling mediates cell fate choice in the zebrafish pronephric duct. PLoS Genetetics 3 (1). https://doi.org/10.1371/journal.pgen.0030018. https://www.ncbi.nlm.nih.gov/pmc/articles/PMC1781496/. (Accessed 31 August 2020).

Magnuson, J.T., Khursigara, A.J., Allmon, E.B., Esbaugh, A.J., Roberts, A.P., 2018. Effects of Deepwater Horizon crude oil on ocular development in two estuarine fish species, red drum (Sciaenops ocellatus) and sheepshead minnow (Cyprinodon variegatus). Ecotoxicol. Environ. Saf. 166, 186–191. https://doi.org/10.1016/j.ecoenv.2018.09.087.

Magnuson, J.T., Bautista, N.M., Lucero, J., Lund, A.K., Xu, E.G., Schlenk, D., Burggren, W.W., Roberts, A.P., 2020. Exposure to crude oil induces retinal apoptosis and impairs visual function in fish. Environ. Sci. Technol. 54 (5), 2843–2850. https://doi.org/10.1021/acs.est.9b07658.

Majumdar, A., Lun, K., Brand, M., Drummond, I.A., 2000. Zebrafish no isthmus reveals a role for pax2.1 in tubule differentiation and patterning events in the pronephric primordia. Development 127 (10), 2089–2098.

McCampbell, K.K., Wingert, R.A., 2014. New tides: using zebrafish to study renal regeneration. Transl. Res. 163 (2), 109–122. https://doi.org/10.1016/j.trsl.2013.10.003.

McDonald, M.D., 2007. The renal contribution to salt and water balance. Fish Osmoregulation. CRC Press 23 p.

McGruer, V., Pasparakis, C., Grosell, M., Stieglitz, J.D., Benetti, D.D., Greer, J.B., Schlenk, D., 2019. Deepwater horizon crude oil exposure alters cholesterol biosynthesis with implications for developmental cardiotoxicity in larval mahi-mahi (Coryphaena hippurus). Comp.Biochem. Physiol.Part C Toxicol.Pharmacol. 220, 31–35. https://doi.org/10.1016/j.cbpc.2019.03.001.

Motamedi, M., Iranmanesh, A., Teimori, A., Soltanian, S., 2020. Effects of toxicity induced by gentamicin on the kidney of killifish Aphaniops hormuzensis and the role of Wt1 and MMP9 genes in response to this toxicity. Jentashapir J. Cell. Mol. Biol. 11 (3). https://doi.org/10.5812/jjcmb.108808. https://sites.kowsarpub.com/jjcmb/articles/108808.html#abstract. (Accessed 26 August 2021).

Nie, M., Blankenship, A.L., Giesy, J.P., 2001. Interactions between aryl hydrocarbon receptor (AhR) and hypoxia signaling pathways. Environ. Toxicol. Pharmacol. 10 (1), 17–27. https://doi.org/10.1016/S1382-6689(01)00065-5.

Outtandy, P., Russell, C., Kleta, R., Bockenhauer, D., 2019. Zebrafish as a model for kidney function and disease. Pediatr. Nephrol. 34 (5), 751–762. https://doi.org/10.1007/s00467-018-3921-7.

Pérez-Rius, C., Castellanos, A., Gaitán-Peñas, H., Navarro, A., Artuch, R., Barrallo-Gimeno, A., Estévez, R., 2019. Role of zebrafish ClC-K/barttin channels in apical kidney chloride reabsorption. J. Physiol. 597 (15), 3969–3983. https://doi.org/10.1113/JP278069.

Perner, B., Englert, C., Bollig, F., 2007. The wilms tumor genes wt1a and wt1b control different steps during formation of the zebrafish pronephros. Dev. Biol. 309 (1), 87–96. https://doi.org/10.1016/j.ydbio.2007.06.022.

Perrichon, P., Le Menach, K., Akcha, F., Cachot, J., Budzinski, H., Bustamante, P., 2016. Toxicity assessment of water-accommodated fractions from two different oils using a zebrafish (Danio rerio) embryo-larval bioassay with a multilevel approach. Sci. Total Environ. 568, 952–966. https://doi.org/10.1016/j.scitotenv.2016.04.186.

Rider, S.A., Tucker, C.S., Rose, K.N., CA, MacRae, Bailey, M.A., Mullins, J.J., del-Pozo, J., 2012. Techniques for the in vivo assessment of cardio-renal function in zebrafish (Danio rerio) larvae. J. Physiol. 590 (Pt 8), 1803–1809. https://doi.org/10.1113/jphysiol.2011.224352.

Rombough, P., 2002. Gills are needed for ionoregulation before they are needed for O2 uptake in developing zebrafish, Danio rerio. J. Exp. Biol. 205 (12), 1787–1794.

Schlenker, L.S., Welch, M.J., Meredith, T.L., Mager, E.M., Lari, E., Babcock, E.A., Pyle, G.G., Munday, P.L., Grosell, M., 2019. Damsels in distress: oil exposure modifies behavior and olfaction in bicolor damselfish (Stegastes partitus). Environ. Sci. Technol. 53 (18), 10993–11001. https://doi.org/10.1021/acs.est.9b03915.

Scholz, H., Kirschner, K., 2011. Oxygen-dependent gene expression in development and cancer: lessons learned from the Wilms' tumor gene, WT1. Front. Mol. Neurosci. 4, 4. https://doi.org/10.3389/fnmol.2011.00004.

Serluca, F.C., Drummond, I.A., Fishman, M.C., 2002. Endothelial signaling in kidney morphogenesis: a role for hemodynamic forces. Curr. Biol. 12 (6), 492–497. https://doi.org/10.1016/s0960-9822(02)00694-2.

Tao, Y., Kim, J., Yin, Y., Zafar, I., Falk, S., He, Z., Faubel, S., Schrier, R.W., Edelstein, C.L., 2007. VEGF receptor inhibition slows the progression of polycystic kidney disease. Kidney Int. 72 (11), 1358–1366. https://doi.org/10.1038/sj.ki.5002550.

Thisse, C., Thisse, B., 2008. High-resolution in situ hybridization to whole-mount zebrafish embryos. Nat. Protoc. 3, 59–69. https://doi.org/10.1038/nprot.2007.514.

Tytler, P., Ireland, J., 2000. The influence of salinity and temperature change on the functioning of the urinary bladder in the early larval stages of the Atlantic herring Clupea harengus L. J. Exp. Biol. 203 (2), 415–422.

Tytler, P., Ireland, J., Fitches, E., 1996. A study of the structure and function of the pronephros in the larvae of the turbot (Scophthalmus maximus) and the herring (Clupea harengus). Mar. Freshw. Behav. Physiol. 28 (1–2), 3–18. https://doi.org/10.1080/10236249609378975.

Vandesompele, J., De Preter, K., Pattyn, F., Poppe, B., Van Roy, N., De Paepe, A., Speleman, F., 2002. Accurate normalization of real-time quantitative RT-PCR data by geometric averaging of multiple internal control genes. Genome Biol. 3 (7). https://doi.org/10.1186/gb-2002-3-7-research0034 research0034.1.

Vasilyev, A., Liu, Y., Mudumana, S., Mangos, S., Lam, P.-Y., Majumdar, A., Zhao, J., Poon, K.-L., Kondrychyn, I., Korzh, V., et al., 2009. Collective cell migration drives morphogenesis of the kidney nephron. PLoS Biology. 7 (1). https://doi.org/10.1371/journal.pbio.1000009. https://www.ncbi.nlm.nih.gov/pmc/articles/PMC2613420/. (Accessed 31 August 2020).

Verschueren, K., 2001. Handbook of Environmental Data on Organic Chemicals. 4th ed. Volumes 1-2. John Wiley & Sons, New York, NY, p. 1756.

Vorrink, S.U., Domann, F.E., 2014. Regulatory crosstalk and interference between the xenobiotic and hypoxia sensing pathways at the AhR-ARNT-HIF1α signaling node. Chem. Biol. Interact. 218, 82–88. https://doi.org/10.1016/j.cbi.2014.05.001.

Weber, S., Taylor, J.C., Winyard, P., Baker, K.F., Sullivan-Brown, J., Schild, R., Knüppel, T., Zurowska, A.M., Caldas-Alfonso, A., Litwin, M., et al., 2008. SIX2 and BMP4 mutations associate with anomalous kidney development. J.Am.Soc.Nephrol. 19 (5), 891–903. https://doi.org/10.1681/ASN.2006111282.

Wingert, R.A., Selleck, R., Yu, J., Song, H.-D., Chen, Z., Song, A., Zhou, Y., Thisse, B., Thisse, C., McMahon, A.P., et al., 2007. The cdx genes and retinoic acid control the positioning and segmentation of the zebrafish pronephros. PLoS Genet. 3 (10), e189. https://doi.org/10.1371/journal.pgen.0030189.

Xu, E.G., Mager, E.M., Grosell, M., Pasparakis, C., Schlenker, L.S., Stieglitz, J.D., Benetti, D., Hazard, E.S., Courtney, S.M., Diamante, G., et al., 2016. Time- and oil-dependent transcriptomic and physiological responses to Deepwater Horizon oil in mahi-mahi (Coryphaena hippurus) embryos and larvae. Environ. Sci. Technol. 50 (14), 7842–7851. https://doi.org/10.1021/acs.est.6b02205.

Xu, E.G., Khursigara, A.J., Magnuson, J., Hazard, E.S., Hardiman, G., Esbaugh, A.J., Roberts, A.P., Schlenk, D., 2017. Larval red drum (Sciaenops ocellatus) sublethal exposure to weathered Deepwater Horizon crude oil: developmental and transcriptomic consequences. Environ. Sci. Technol. 51 (17), 10162–10172. https://doi.org/10.1021/acs.est.7b02037.

Yang, C., Boucher, F., Tremblay, A., Michaud, J.L., 2004. Regulatory interaction between arylhydrocarbon receptor and SIM1, two basic helix-loop-helix PAS proteins involved in the control of food intake. J. Biol. Chem. 279 (10), 9306–9312. https://doi.org/10.1074/jbc.M307927200.

Zhang, Y., Huang, L., Wang, C., Gao, D., Zuo, Z., 2013. Phenanthrene exposure produces cardiac defects during embryo development of zebrafish (Danio rerio) through activation of MMP-9. Chemosphere 93 (6), 1168–1175. https://doi.org/10.1016/j.chemosphere.2013.06.056.

Zhao, S., Fernald, R.D., 2005. Comprehensive algorithm for quantitative real-time polymerase chain reaction. J. Comput. Biol. 12 (8), 1047–1064. https://doi.org/10.1089/cmb.2005.12.1047.